Journal of Computational and Applied Mathematics 368 (2020) 112453

Contents lists available at ScienceDirect

Journal of Computational and Applied Mathematics

journal homepage: www.elsevier.com/locate/cam

Analysis and application of the interpolating element free Galerkin (IEFG) method to simulate the prevention of groundwater contamination with application in fluid flow

Mostafa Abbaszadeh [a,*], Mehdi Dehghan [a], Amirreza Khodadadian [c,d], Clemens Heitzinger [c,b]

[a] Department of Applied Mathematics, Faculty of Mathematics and Computer Sciences, Amirkabir University of Technology, No. 424, Hafez Ave., 15914 Tehran, Iran
[b] School of Mathematical and Statistical Sciences, Arizona State University, Tempe, AZ 85287, USA
[c] Institute for Analysis and Scientific Computing, Vienna University of Technology (TU Wien), Wiedner Hauptstraße 8–10, 1040 Vienna, Austria
[d] Leibniz University of Hanover, Institute for Applied Mathematics, Welfengarten 1, 30167, Hanover, Germany

ARTICLE INFO

Article history:
Received 11 January 2019
Received in revised form 8 May 2019

MSC:
65M70
34A34

Keywords:
Groundwater equation and fluid flow
Prevention of groundwater contamination
Element free Galerkin (EFG) method
Interpolating MLS
Unconditionally stable
Convergence

ABSTRACT

We develop a meshless numerical procedure to simulate the groundwater equation (GWE). The used technique is based on the interpolating element free Galerkin (IEFG) method. The interpolating moving least squares (IMLS) approximation produces a set of functions such that they are well-known as "*shape functions*". The IEFG technique employs the shape functions of IMLS approximation. The shape functions of IMLS approximation vanish on the boundary and also they satisfy the property of the Kronecker Delta function. Thus, Dirichlet boundary conditions can be exactly imposed. In this paper, we check the unconditional stability and convergence of the proposed numerical scheme based on the energy method. The numerical results confirm the theoretical analysis.

1. Introduction

The EFG technique was introduced by Belytschko [1–3]. The EFG and IEFG techniques and also their modifications as two numerical procedures have been used for solving different linear and non-linear PDEs. For example the interpolating EFG technique is based on the interpolating moving least squares approximation. The IMLS was developed by Lancaster and Salkauskas [4]. Authors of [5] proposed a simple way to construct the shape function of interpolating MLS. Also, they proposed an improved boundary element-free method (IBEFM) for solving two-dimensional potential problems [5]. Furthermore, the main aim of [6] is the use of the revised interpolating MLS shape functions in the boundary element procedure to simulate 2D elasticity models. The main purpose of [7,8] is to propound an improved IMLS for solving 2D elasticity and potential problems. Authors of [9] developed an error estimation for the IMLS that is presented by Lancaster and Salkauskas [4]. The error estimate of the approximation function and its first and second order derivatives of the IMLS

* Corresponding author.
E-mail addresses: m.abbaszadeh@aut.ac.ir (M. Abbaszadeh), mdehghan@aut.ac.ir, mdehghan.aut@gmail.com (M. Dehghan), amirreza.khodadadian@tuwien.ac.at (A. Khodadadian), clemens.heitzinger@tuwien.ac.at (C. Heitzinger).

https://doi.org/10.1016/j.cam.2019.112453
0377-0427/

method are developed in [10] based on the n-dimensional space. Authors of [11] proposed a new method for deriving the IMLS approximation and they developed the complex variable MLS (CVMLS) approximation with error estimate.

Authors of [12] employed the IMLS method to present a novel IEFG method for solving two-dimensional elastoplasticity models. The IMLS approximation in the complex sense was developed in [13] to simulate the temperature field problems. Furthermore, the IMLS technique has been used in [14] to solve nonlinear elastic models. The main target of [15] is to expand a new meshless technique using the boundary integral equation for solving 2D elastodynamic models. The main target of [16] is to explain the complex variable reproducing kernel particle method (CVRKPM) for solving the bending problems of isotropic thin plates on elastic foundations. In [17], the authors presented the dimension split element-free Galerkin (DSEFG) method for three-dimensional potential problems. The moving Kriging element-free Galerkin method has been combined in [18] with the variational multiscale algorithm to obtain acceptable and high-resolution solutions. The proposed technique in [18] is tested for some PDEs with discontinuous solution such as Burgers, Sods shock tube, advection-reaction-diffusion, Kuramoto-Sivashinsky, Boussinesq and shallow water equations.

The main aim of [19] is to propose the interpolating moving least-squares (IMLS) method based on a nonsingular weight function to obtain the approximation function then the improved element-free Galerkin (IEFG) method based on a nonsingular weight function for solving elastic large deformation problems is presented. The interpolating moving least-squares (IMLS) method based on a nonsingular weight function is proposed in [20] to construct the approximation function to simulate the problem of inhomogeneous swelling of polymer gels. Authors of [21] developed the interpolating EFG method based on a nonsingular weight function for solving elastoplastic large deformation problems.

Interpolating EFG method has been constructed by many researchers such as 2D elastoplasticity problems [12,22], 2D potential problems [23,24], 2D large deformation problems [25], 2D transient heat conduction problems [26], incompressible Navier–Stokes equation [27,28], 2D Schrödinger equation [29], biological populations [30], two-dimensional large deformation of inhomogeneous swelling of gels [31], etc. Authors of [32] analyzed properties, stability and error of the MLS approximation and also to overcome the inherent instability, a stabilized approximation is developed and analyzed. The main aim of [33] is to develop the interpolating stabilized EFG method for solving a neutral delay PDE with fractional derivative in terms of Caputo fractional derivatives. Authors of [34] proposed a new numerical method based on the interpolating element free Galerkin method for solving a class of wave models, i.e., the Korteweg–de Vries–Rosenau-regularized long-wave equation with application in plasma physics. Error analysis and numerical simulation of magnetohydrodynamics (MHD) equation based on the interpolating element free Galerkin method are developed in [35]. The main aim of [36] is to propose a new truly meshless numerical technique based on the interpolating MLS approximation to solve the one-and two-dimensional elliptic interface problems. The two-grid procedure has been combined in [37] with the interpolating element free Galerkin method for solving nonlinear Rosenau-regularized long wave (RRLW) equation with error analysis. Authors of [38] applied a finite element scheme and interpolating element free Galerkin technique for the numerical solution of the two-dimensional time fractional diffusion-wave equation on the irregular domains. An upwind local radial basis functions-differential quadrature (RBF-DQ) method with proper orthogonal decomposition (POD) approach is presented in [39] for solving compressible Euler equation. Also the interested reader can refer to [40–42] for alternative approaches in improving the moving least squares approximation. The main aim of [43] is to explore the application of the meshless local radial basis function collocation method (LRBFCM) for the solution of coupled heat transfer and fluid flow problems with a free surface. An interpolating element-free Galerkin scaled boundary method is developed in [44] for analyzing steady heat conduction problems. Authors of [45] proposed an explicit local radial basis function collocation method to simulate of laminar backward facing step flow under magnetic field.

1.1. Governing model

The 2D groundwater equation (GWE) is [46,47]

$$\begin{cases} u_t + \mu\nabla u - \nabla\cdot(D\nabla u) + \varpi_p p_1 f(u,v) = 0, \\ v_t + \mu\nabla v - \nabla\cdot(D\nabla v) + \varpi_p p_2 g(u,v) = 0, \\ w_t + \mu\nabla w - \nabla\cdot(D\nabla w) + \varpi_p p_3 h(u,v) = 0, \end{cases} \tag{1.1}$$

in which u, v and w denote the concentrations of the main ground substance, aqueous solution electrolyte and microorganism, respectively [46,47]. Also, the nonlinear terms are

$$f(u,v) = g(u,v) = h(u,v) = \frac{u}{\kappa_1 + u} + \frac{v}{\kappa_2 + v},$$

and μ and D are constants. Most real world problems can be modeled by the nonlinear PDEs [48,49]. The groundwater model is one of the nonlinear equations to describe prevention of the groundwater contaminant [47]. Several scholars investigated Eq. (1.1) for example improved finite volume approach [47], meshless local approaches [50,51], lattice Boltzmann technique [52], a front-tracking method [53], the novel WENO methods [54], a finite element method [55], etc. The interested readers can refer to [56,57] to obtain more information about Eq. (1.1). A new laboratory dataset on the moisture-pressure relationship above a dispersive groundwater wave in a two-dimensional vertical unconfined sand flume aquifer driven by simple harmonic forcing is presented in [58].

2. Time-discrete formula

We define $t_k = kdt$ for $k = 0, 1, \ldots, N$, where $dt = T/N$. Let

$$v^{n-\frac{1}{2}} = v(x, y, t_{n-\frac{1}{2}}) = \frac{1}{2}\left(v^n + v^{n-1}\right), \qquad \delta_t v^{n-\frac{1}{2}} = \frac{1}{dt}\left(v^n - u^{n-1}\right), \qquad v^n = v(x, y, t_n).$$

Applying the Crank-Nicolson idea to Eq. (1.1), yields

$$\begin{cases} \dfrac{\partial u^{n-\frac{1}{2}}}{\partial t} + \mu\nabla u^{n-\frac{1}{2}} - \nabla\cdot\left(D\nabla u^{n-\frac{1}{2}}\right) + \varpi_p p_1 f\left(u^{n-\frac{1}{2}}, v^{n-\frac{1}{2}}\right) = 0, \\ \dfrac{\partial v^{n-\frac{1}{2}}}{\partial t} + \mu\nabla v^{n-\frac{1}{2}} - \nabla\cdot\left(D\nabla v^{n-\frac{1}{2}}\right) + \varpi_p p_2 g\left(u^{n-\frac{1}{2}}, v^{n-\frac{1}{2}}\right) = 0, \\ \dfrac{\partial w^{n-\frac{1}{2}}}{\partial t} + \mu\nabla w^{n-\frac{1}{2}} - \nabla\cdot\left(D\nabla w^{n-\frac{1}{2}}\right) + \varpi_p p_3 h\left(u^{n-\frac{1}{2}}, v^{n-\frac{1}{2}}\right) + r(\boldsymbol{x}) w^{n-\frac{1}{2}} = 0. \end{cases} \tag{2.1}$$

Simplifying relation (2.1) yields

$$\begin{cases} \dfrac{u^n - u^{n-1}}{dt} + \mu\left[\dfrac{\nabla u^n + \nabla u^{n-1}}{2}\right] - \nabla\cdot\left[D\left(\dfrac{\nabla u^n + \nabla u^{n-1}}{2}\right)\right] + \varpi_p p_1 f\left(u^{n-\frac{1}{2}}, v^{n-\frac{1}{2}}\right) = 0, \\ \dfrac{v^n - v^{n-1}}{dt} + \mu\left[\dfrac{\nabla v^n + \nabla v^{n-1}}{2}\right] - \nabla\cdot\left[D\left(\dfrac{\nabla v^n + \nabla v^{n-1}}{2}\right)\right] + \varpi_p p_2 g\left(u^{n-\frac{1}{2}}, v^{n-\frac{1}{2}}\right) = 0, \\ \dfrac{w^n - w^{n-1}}{dt} + \mu\left[\dfrac{\nabla w^n + \nabla w^{n-1}}{2}\right] - \nabla\cdot\left[D\left(\dfrac{\nabla w^n + \nabla w^{n-1}}{2}\right)\right] \\ \qquad + \varpi_p p_3 h\left(u^{n-\frac{1}{2}}, v^{n-\frac{1}{2}}\right) + r(\boldsymbol{x})\left[\dfrac{w^n + w^{n-1}}{2}\right] = 0, \end{cases} \tag{2.2}$$

such that by linearization of Eq. (2.2), we find

$$\begin{cases} u^n + \dfrac{dt}{2}\mu\nabla u^n - \dfrac{dt}{2}\nabla\cdot\left[D\nabla u^n\right] \\ \qquad = u^{n-1} - \dfrac{dt}{2}\mu\nabla u^{n-1} + \dfrac{dt}{2}\nabla\cdot\left[D\nabla u^{n-1}\right] - dt\varpi_p p_1 f\left(u^{n-1}, v^{n-1}\right), \\ v^n + \dfrac{dt}{2}\mu\nabla v^n - \dfrac{dt}{2}\nabla\cdot\left[D\nabla v^n\right] \\ \qquad = v^{n-1} - \dfrac{dt}{2}\mu\nabla v^{n-1} + \dfrac{dt}{2}\nabla\cdot\left[D\nabla v^{n-1}\right] - dt\varpi_p p_2 g\left(u^{n-1}, v^{n-1}\right), \\ \left(1 + \dfrac{dt}{2}r(\boldsymbol{x})\right) w^n + \frac{dt}{2}\mu\nabla w^n - \frac{dt}{2}\nabla\cdot[D\nabla w^n] \\ \qquad = \left(1 - \dfrac{dt}{2}r(\boldsymbol{x})\right) w^{n-1} - \dfrac{dt}{2}\mu\nabla w^{n-1} + \dfrac{dt}{2}\nabla\cdot\left[D\nabla w^{n-1}\right] - dt\varpi_p p_3 h\left(u^{n-1}, v^{n-1}\right). \end{cases} \tag{2.3}$$

The vector–matrix form of (2.3) is

$$\begin{aligned} &\begin{bmatrix} 1 & 0 & 0 \\ 0 & 1 & 0 \\ 0 & 0 & \left(1 + \frac{dt}{2}r(\boldsymbol{x})\right) \end{bmatrix}\begin{bmatrix} u^n \\ v^n \\ w^n \end{bmatrix} + \frac{dt}{2}\begin{bmatrix} 1 & 0 & 0 \\ 0 & 1 & 0 \\ 0 & 0 & 1 \end{bmatrix}\nabla\begin{bmatrix} u^n \\ v^n \\ w^n \end{bmatrix} \\ &- \frac{dt}{2}\begin{bmatrix} 1 & 0 & 0 \\ 0 & 1 & 0 \\ 0 & 0 & 1 \end{bmatrix}\nabla\cdot D\nabla\begin{bmatrix} u^n \\ v^n \\ w^n \end{bmatrix} = \begin{bmatrix} 1 & 0 & 0 \\ 0 & 1 & 0 \\ 0 & 0 & \left(1 - \frac{dt}{2}r(\boldsymbol{x})\right) \end{bmatrix}\begin{bmatrix} u^{n-1} \\ v^{n-1} \\ w^{n-1} \end{bmatrix} \\ &- \frac{dt}{2}\begin{bmatrix} 1 & 0 & 0 \\ 0 & 1 & 0 \\ 0 & 0 & 1 \end{bmatrix}\nabla\begin{bmatrix} u^{n-1} \\ v^{n-1} \\ w^{n-1} \end{bmatrix} + \frac{dt}{2}\begin{bmatrix} 1 & 0 & 0 \\ 0 & 1 & 0 \\ 0 & 0 & 1 \end{bmatrix}\nabla\cdot D\nabla\begin{bmatrix} u^{n-1} \\ v^{n-1} \\ w^{n-1} \end{bmatrix} \\ &- dt\begin{bmatrix} \varpi_p p_1 & 0 & 0 \\ 0 & \varpi_p p_2 & 0 \\ 0 & 0 & \varpi_p p_3 \end{bmatrix}\begin{bmatrix} f\left(u^{n-1}, v^{n-1}\right) \\ g\left(u^{n-1}, v^{n-1}\right) \\ h\left(u^{n-1}, v^{n-1}\right) \end{bmatrix}, \end{aligned} \tag{2.4}$$

or equivalently

$$\boldsymbol{M}_1\boldsymbol{U}^n+\frac{dt}{2}\boldsymbol{I}\nabla\boldsymbol{U}^n-\frac{dt}{2}\boldsymbol{I}\nabla\cdot D\nabla\boldsymbol{U}^n=\boldsymbol{M}_2\boldsymbol{U}^{n-1}-\frac{dt}{2}\boldsymbol{I}\nabla\boldsymbol{U}^{n-1}+\frac{dt}{2}\boldsymbol{I}\nabla\cdot D\nabla\boldsymbol{U}^{n-1}-dt\boldsymbol{N}\boldsymbol{F}\left(\boldsymbol{U}^{n-1}\right), \tag{2.5}$$

in which

$$\boldsymbol{M}_1=\begin{bmatrix}1&0&0\\0&1&0\\0&0&\left(1+\frac{dt}{2}r(\boldsymbol{x})\right)\end{bmatrix},\quad \boldsymbol{M}_2=\begin{bmatrix}1&0&0\\0&1&0\\0&0&\left(1-\frac{dt}{2}r(\boldsymbol{x})\right)\end{bmatrix},$$
$$\boldsymbol{I}=\begin{bmatrix}1&0&0\\0&1&0\\0&0&1\end{bmatrix},\quad \boldsymbol{N}=\begin{bmatrix}w_pe_1&0&0\\0&w_pe_2&0\\0&0&w_pe_3\end{bmatrix}. \tag{2.6}$$

2.1. Analytical investigation for difference scheme (2.5)

In the current study, we want to analytically check the temporal discretization. In the error estimations, we assume that $r(\boldsymbol{x})$ is a positive constant.

Theorem 2.1. *Let $\boldsymbol{U}^n\in\boldsymbol{H}_0^1(\Omega)$. Then relation (2.5) is unconditionally stable.*

Proof. The corresponding weak form for Eq. (2.5) is:
Find $u^n\in H_0^1(\Omega)$ **such that**

$$\begin{aligned}\boldsymbol{M}_1\left\langle\boldsymbol{U}^n,\boldsymbol{V}\right\rangle&+\frac{dt}{2}\boldsymbol{I}\left\langle D\nabla\boldsymbol{U}^n,\nabla\boldsymbol{V}\right\rangle-\frac{dt}{2}\boldsymbol{I}\left\langle\boldsymbol{U}^n,\frac{\partial}{\partial x}\boldsymbol{V}\right\rangle-\frac{dt}{2}\boldsymbol{I}\left\langle\boldsymbol{U}^n,\frac{\partial}{\partial y}\boldsymbol{V}\right\rangle\\&=\boldsymbol{M}_2\left\langle\boldsymbol{U}^{n-1},\boldsymbol{V}\right\rangle-\frac{dt}{2}\boldsymbol{I}\left\langle D\nabla\boldsymbol{U}^{n-1},\nabla\boldsymbol{V}\right\rangle+\frac{dt}{2}\boldsymbol{I}\left\langle\boldsymbol{U}^{n-1},\frac{\partial}{\partial x}\boldsymbol{V}\right\rangle\\&+\frac{dt}{2}\boldsymbol{I}\left\langle\boldsymbol{U}^{n-1},\frac{\partial}{\partial y}\boldsymbol{V}\right\rangle-dt\boldsymbol{N}\left\langle\boldsymbol{F},\boldsymbol{V}\right\rangle,\qquad\forall\quad\boldsymbol{V}\in\boldsymbol{H}_0^1(\Omega).\end{aligned} \tag{2.7}$$

Let $\widetilde{\boldsymbol{U}}^n$ be an approximate solution of $\boldsymbol{U}^n$, then

$$\begin{aligned}\boldsymbol{M}_1\left\langle\widetilde{\boldsymbol{U}}^n,\boldsymbol{V}\right\rangle&+\frac{dt}{2}\boldsymbol{I}\left\langle D\nabla\widetilde{\boldsymbol{U}}^n,\nabla\boldsymbol{V}\right\rangle-\frac{dt}{2}\boldsymbol{I}\left\langle\widetilde{\boldsymbol{U}}^n,\frac{\partial}{\partial x}\boldsymbol{V}\right\rangle-\frac{dt}{2}\boldsymbol{I}\left\langle\boldsymbol{U}^n,\frac{\partial}{\partial y}\boldsymbol{V}\right\rangle\\&=\boldsymbol{M}_2\left\langle\widetilde{\boldsymbol{U}}^{n-1},\boldsymbol{V}\right\rangle-\frac{dt}{2}\boldsymbol{I}\left\langle D\nabla\widetilde{\boldsymbol{U}}^{n-1},\nabla\boldsymbol{V}\right\rangle+\frac{dt}{2}\boldsymbol{I}\left\langle\widetilde{\boldsymbol{U}}^{n-1},\frac{\partial}{\partial x}\boldsymbol{V}\right\rangle\\&+\frac{dt}{2}\boldsymbol{I}\left\langle\widetilde{\boldsymbol{U}}^{n-1},\frac{\partial}{\partial y}\boldsymbol{V}\right\rangle-dt\boldsymbol{N}\left\langle\widetilde{\boldsymbol{F}},\boldsymbol{V}\right\rangle,\qquad\forall\quad\boldsymbol{V}\in\boldsymbol{H}_0^1(\Omega),\end{aligned} \tag{2.8}$$

in which $\widetilde{\boldsymbol{F}}=\boldsymbol{F}(\widetilde{\boldsymbol{U}})$. Subtracting Eq. (2.8) from Eq. (2.7) results in

$$\begin{aligned}\boldsymbol{M}_1\left\langle\boldsymbol{\Theta}^n,\boldsymbol{V}\right\rangle&+\frac{dt}{2}\boldsymbol{I}\left\langle D\nabla\boldsymbol{\Theta}^n,\nabla\boldsymbol{V}\right\rangle-\frac{dt}{2}\boldsymbol{I}\left\langle\boldsymbol{\Theta}^n,\frac{\partial}{\partial x}\boldsymbol{V}\right\rangle-\frac{dt}{2}\boldsymbol{I}\left\langle\boldsymbol{\Theta}^n,\frac{\partial}{\partial y}\boldsymbol{V}\right\rangle\\&=\boldsymbol{M}_2\left\langle\boldsymbol{\Theta}^{n-1},\boldsymbol{V}\right\rangle-\frac{dt}{2}\boldsymbol{I}\left\langle D\nabla\boldsymbol{\Theta}^{n-1},\nabla\boldsymbol{V}\right\rangle+\frac{dt}{2}\boldsymbol{I}\left\langle\boldsymbol{\Theta}^{n-1},\frac{\partial}{\partial x}\boldsymbol{V}\right\rangle\\&+\frac{dt}{2}\boldsymbol{I}\left\langle\boldsymbol{\Theta}^{n-1},\frac{\partial}{\partial y}\boldsymbol{V}\right\rangle-dt\boldsymbol{N}\left\langle\boldsymbol{F}-\widetilde{\boldsymbol{F}},\boldsymbol{V}\right\rangle,\qquad\forall\quad\boldsymbol{V}\in\boldsymbol{H}_0^1(\Omega),\end{aligned} \tag{2.9}$$

in which

$$\boldsymbol{\Theta}^n=\boldsymbol{U}^n-\widetilde{\boldsymbol{U}}^n.$$

Setting $\boldsymbol{V}=\boldsymbol{\Theta}^n$ in Eq. (2.9) yields

$$\begin{aligned}\boldsymbol{M}_1\left\langle\boldsymbol{\Theta}^n,\boldsymbol{\Theta}^n\right\rangle&+\frac{dt}{2}\boldsymbol{I}\left\langle D\nabla\boldsymbol{\Theta}^n,\nabla\boldsymbol{\Theta}^n\right\rangle-\frac{dt}{2}\boldsymbol{I}\left\langle\boldsymbol{\Theta}^n,\frac{\partial}{\partial x}\boldsymbol{\Theta}^n\right\rangle-\frac{dt}{2}\boldsymbol{I}\left\langle\boldsymbol{\Theta}^n,\frac{\partial}{\partial y}\boldsymbol{\Theta}^n\right\rangle\\&=\boldsymbol{M}_2\left\langle\boldsymbol{\Theta}^{n-1},\boldsymbol{\Theta}^n\right\rangle-\frac{dt}{2}\boldsymbol{I}\left\langle D\nabla\boldsymbol{\Theta}^{n-1},\nabla\boldsymbol{\Theta}^n\right\rangle+\frac{dt}{2}\boldsymbol{I}\left\langle\boldsymbol{\Theta}^{n-1},\frac{\partial}{\partial x}\boldsymbol{\Theta}^n\right\rangle\\&+\frac{dt}{2}\boldsymbol{I}\left\langle\boldsymbol{\Theta}^{n-1},\frac{\partial}{\partial y}\boldsymbol{\Theta}^n\right\rangle-dt\boldsymbol{N}\left\langle\boldsymbol{F}-\widetilde{\boldsymbol{F}},\boldsymbol{\Theta}^n\right\rangle.\end{aligned} \tag{2.10}$$

Using the Cauchy-Schwarz inequality, Eq. (2.10) yields

$$\begin{aligned}\boldsymbol{M}_1 \left\| \boldsymbol{\Theta}^n \right\|^2_{\boldsymbol{L}^2(\Omega)} + \frac{dt}{2} \|D\| \left\| \nabla \boldsymbol{\Theta}^n \right\|^2_{\boldsymbol{L}^2(\Omega)} \leq \frac{dt}{2} \left\langle \boldsymbol{\Theta}^n, \frac{\partial}{\partial x} \boldsymbol{\Theta}^n \right\rangle + \frac{dt}{2} \left\langle \boldsymbol{\Theta}^n, \frac{\partial}{\partial y} \boldsymbol{\Theta}^n \right\rangle \\ + \boldsymbol{M}_2 \left\| \boldsymbol{\Theta}^n \right\|_{\boldsymbol{L}^2(\Omega)} \left\| \boldsymbol{\Theta}^{n-1} \right\|_{\boldsymbol{L}^2(\Omega)} + \frac{dt}{2} \|D\| \left\| \nabla \boldsymbol{\Theta}^n \right\|_{\boldsymbol{L}^2(\Omega)} \left\| \nabla \boldsymbol{\Theta}^{n-1} \right\|_{\boldsymbol{L}^2(\Omega)} \\ + \frac{dt}{2} \left\langle \boldsymbol{\Theta}^{n-1}, \frac{\partial}{\partial y} \boldsymbol{\Theta}^n \right\rangle + \frac{dt}{2} \left\langle \boldsymbol{\Theta}^{n-1}, \frac{\partial}{\partial x} \boldsymbol{\Theta}^n \right\rangle - dt \boldsymbol{N} \left\langle \boldsymbol{F} - \widetilde{\boldsymbol{F}}, \boldsymbol{\Theta}^n \right\rangle.\end{aligned}$$

There exists a constant $\boldsymbol{L}$

$$\left\| \boldsymbol{F} - \widetilde{\boldsymbol{F}} \right\| \leq \boldsymbol{L} \boldsymbol{\Theta}^{n-1}. \tag{2.11}$$

By simplification we have

$$\begin{aligned}\boldsymbol{M}_1 \left\| \boldsymbol{\Theta}^n \right\|^2_{\boldsymbol{L}^2(\Omega)} + \frac{dt}{2} \|D\| \left\| \nabla \boldsymbol{\Theta}^n \right\|^2_{\boldsymbol{L}^2(\Omega)} \leq \frac{dt}{2} \left\| \boldsymbol{\Theta}^n \right\|_{\boldsymbol{L}^2(\Omega)} \left\| \nabla \boldsymbol{\Theta}^n \right\|_{\boldsymbol{L}^2(\Omega)} + \frac{dt}{2} \left\| \boldsymbol{\Theta}^{n-1} \right\|_{\boldsymbol{L}^2(\Omega)} \left\| \nabla \boldsymbol{\Theta}^n \right\|_{\boldsymbol{L}^2(\Omega)} \\ + \boldsymbol{M}_2 \left\| \boldsymbol{\Theta}^n \right\|_{\boldsymbol{L}^2(\Omega)} \left\| \boldsymbol{\Theta}^{n-1} \right\|_{\boldsymbol{L}^2(\Omega)} + \frac{dt}{2} \|D\| \left\| \nabla \boldsymbol{\Theta}^n \right\|_{\boldsymbol{L}^2(\Omega)} \left\| \nabla \boldsymbol{\Theta}^{n-1} \right\|_{\boldsymbol{L}^2(\Omega)} \\ + dt \boldsymbol{L} \boldsymbol{N} \left\| \boldsymbol{\Theta}^{n-1} \right\|_{\boldsymbol{L}^2(\Omega)} \left\| \boldsymbol{\Theta}^n \right\|_{\boldsymbol{L}^2(\Omega)}.\end{aligned}$$

So, from the assumption

$$\boldsymbol{M}_2(i,j) \leq \boldsymbol{M}_1(i,j), \qquad i,j = 1,2,3,$$

we can find

$$\begin{aligned}\frac{1}{2}\boldsymbol{M}_1 \left\| \boldsymbol{\Theta}^n \right\|^2_{\boldsymbol{L}^2(\Omega)} + \frac{dt}{4} \|D\| \left\| \nabla \boldsymbol{\Theta}^n \right\|^2_{\boldsymbol{L}^2(\Omega)} \\ \leq \frac{1}{2}\boldsymbol{M}_1 \left\| \boldsymbol{\Theta}^{n-1} \right\|^2_{\boldsymbol{L}^2(\Omega)} + \frac{dt}{4} \|D\| \left\| \nabla \boldsymbol{\Theta}^{n-1} \right\|^2_{\boldsymbol{L}^2(\Omega)} \\ + \frac{\boldsymbol{C_1} \boldsymbol{L} dt}{2\|D\|} \left\| \boldsymbol{\Theta}^n \right\|^2_{\boldsymbol{L}^2(\Omega)} + \frac{\boldsymbol{C_2} \boldsymbol{L} dt}{2\|D\|} \left\| \boldsymbol{\Theta}^{n-1} \right\|^2_{\boldsymbol{L}^2(\Omega)} \\ + \frac{dt}{2} C_\Omega \left\| \nabla \boldsymbol{\Theta}^n \right\|^2_{\boldsymbol{L}^2(\Omega)} + \frac{dt}{4} C_\Omega \left\| \nabla \boldsymbol{\Theta}^{n-1} \right\|^2_{\boldsymbol{L}^2(\Omega)} + \frac{dt}{4} C_\Omega \left\| \nabla \boldsymbol{\Theta}^n \right\|^2_{\boldsymbol{L}^2(\Omega)}.\end{aligned} \tag{2.12}$$

By defining the weighted norm

$$\left\| \boldsymbol{\Theta}^n \right\|^2_{\boldsymbol{H}_w(\Omega)} = \boldsymbol{M}_1 \left\| \boldsymbol{\Theta}^n \right\|^2_{\boldsymbol{L}^2(\Omega)} + \frac{1}{2} dt \|D\| \left\| \nabla \boldsymbol{\Theta}^n \right\|^2_{\boldsymbol{L}^2(\Omega)},$$

Eq. (2.12) can be changed to

$$\left\| \boldsymbol{\Theta}^n \right\|^2_{\boldsymbol{H}_w(\Omega)} \leq \left\| \boldsymbol{\Theta}^{n-1} \right\|^2_{\boldsymbol{H}_w(\Omega)} + \frac{\boldsymbol{C_1} \boldsymbol{L} dt}{\|D\|} \left\| \boldsymbol{\Theta}^n \right\|^2_{\boldsymbol{H}_w(\Omega)} + \frac{\boldsymbol{C_2} \boldsymbol{L} dt}{\|D\|} \left\| \boldsymbol{\Theta}^{n-1} \right\|^2_{\boldsymbol{H}_w(\Omega)} + dt C_\Omega \left\| \nabla \boldsymbol{\Theta}^n \right\|^2_{\boldsymbol{L}^2(\Omega)}. \tag{2.13}$$

From Eq. (2.13), we obtain

$$\begin{aligned}\sum_{m=1}^{n} \left\| \boldsymbol{\Theta}^m \right\|^2_{\boldsymbol{H}_w(\Omega)} \leq \sum_{m=1}^{n} \left\| \boldsymbol{\Theta}^{m-1} \right\|^2_{\boldsymbol{H}_w(\Omega)} + \frac{\boldsymbol{C_1} \boldsymbol{L} dt}{\|D\|} \sum_{m=1}^{n} \left\| \boldsymbol{\Theta}^m \right\|^2_{\boldsymbol{H}_w(\Omega)} \\ + \frac{\boldsymbol{C_2} \boldsymbol{L} dt}{\|D\|} \sum_{m=1}^{n} \left\| \boldsymbol{\Theta}^{m-1} \right\|^2_{\boldsymbol{H}_w(\Omega)} + dt C_\Omega \sum_{m=1}^{n} \left\| \nabla \boldsymbol{\Theta}^m \right\|^2_{\boldsymbol{L}^2(\Omega)}.\end{aligned} \tag{2.14}$$

Thus, we have

$$\left\| \boldsymbol{\Theta}^n \right\|^2_{\boldsymbol{H}_w(\Omega)} \leq \left\| \boldsymbol{\Theta}^0 \right\|^2_{\boldsymbol{H}_w(\Omega)} + \frac{2\boldsymbol{C}\boldsymbol{L} dt}{\|D\|} \sum_{m=1}^{n} \left\| \boldsymbol{\Theta}^m \right\|^2_{\boldsymbol{H}_w(\Omega)} + dt C_\Omega \sum_{m=1}^{n} \left\| \nabla \boldsymbol{\Theta}^m \right\|^2_{\boldsymbol{L}^2(\Omega)}. \tag{2.15}$$

Applying the Gronwall Lemma to Eq. (2.15) results in

$$\begin{aligned}\left\| \boldsymbol{\Theta}^n \right\|^2_{\boldsymbol{H}_w(\Omega)} &\leq \left\| \boldsymbol{\Theta}^0 \right\|^2_{\boldsymbol{H}_w(\Omega)} + dt C_\Omega \sum_{m=1}^{n} \left\| \nabla \boldsymbol{\Theta}^m \right\|^2_{\boldsymbol{L}^2(\Omega)} + \frac{2\boldsymbol{C}\boldsymbol{L} dt}{\|D\|} \sum_{m=1}^{n} \left\| \boldsymbol{\Theta}^m \right\|^2_{\boldsymbol{H}_w(\Omega)} \\ &\leq \left\{ \left\| \boldsymbol{\Theta}^0 \right\|^2_{\boldsymbol{H}_w(\Omega)} + dt C_\Omega \sum_{m=1}^{n} \left\| \nabla \boldsymbol{\Theta}^m \right\|^2_{\boldsymbol{L}^2(\Omega)} \right\} \exp\left(\frac{2\boldsymbol{C}\boldsymbol{L} n dt}{\|D\|} \right).\end{aligned}$$

So it can be seen that

$$\left\| \boldsymbol{\Theta}^n \right\|_{\boldsymbol{L}^2(\Omega)} \leq \left\| \boldsymbol{\Theta}^n \right\|_{\boldsymbol{H}_w(\Omega)} \leq \boldsymbol{C} \left\{ \left\| \boldsymbol{\Theta}^0 \right\|^2_{\boldsymbol{H}_w(\Omega)} + dt C_\Omega \sum_{m=1}^{n} \left\| \nabla \boldsymbol{\Theta}^m \right\|^2_{\boldsymbol{L}^2(\Omega)} \right\}.$$

We know that in $H_0^k(\Omega)$ the norm $\|\bullet\|_{L^k(\Omega)}$ and the seminorm $|\bullet|_{H^k(\Omega)}$ are equivalent, so it can be seen

$$\begin{aligned}\left\|\boldsymbol{\Theta}^n\right\|^2_{\boldsymbol{L}^2(\Omega)} &\leq \mathbf{C}\left\{\left\|\boldsymbol{\Theta}^0\right\|^2_{\boldsymbol{H}_w(\Omega)} + dtC_\Omega \sum_{m=1}^{n}\left\|\nabla\boldsymbol{\Theta}^m\right\|^2_{\boldsymbol{L}^2(\Omega)}\right\}\\ &= \mathbf{C}\left\{\left\|\boldsymbol{\Theta}^0\right\|^2_{\boldsymbol{H}_w(\Omega)} + dtC_\Omega \sum_{m=1}^{n}\left|\boldsymbol{\Theta}^m\right|^2_{\boldsymbol{H}^1(\Omega)}\right\}\\ &\leq \mathbf{C}_1^*\left\{\left\|\Theta^0\right\|^2_{\boldsymbol{H}_w(\Omega)} + dtC_\Omega \sum_{m=1}^{n}\left\|\boldsymbol{\Theta}^m\right\|^2_{\boldsymbol{L}^2(\Omega)}\right\}\\ &\leq \mathbf{C}_1^*\left\|\boldsymbol{\Theta}^0\right\|^2_{\boldsymbol{H}_w(\Omega)}\exp\left(C_\Omega T\right),\end{aligned} \tag{2.16}$$

which completes the proof. ■

Theorem 2.2. *The semi-discrete scheme (2.5) has the convergence order $\mathcal{O}(dt)$.*

Proof. Let define

$$\boldsymbol{\Xi}^n = \boldsymbol{u}^n - \boldsymbol{U}^n, \qquad n \geq 1,$$

where $\boldsymbol{\Xi}^0 = \mathbf{0}$. Then, the round off error is

$$\begin{aligned}&\boldsymbol{M}_1\boldsymbol{\Xi}^n + \frac{dt}{2}\boldsymbol{I}\nabla\cdot\zeta(\boldsymbol{x})\nabla\boldsymbol{\Xi}^n - \frac{dt}{2}\boldsymbol{I}\nabla\cdot\zeta(\boldsymbol{x})\nabla\boldsymbol{\Xi}^n =\\ &\boldsymbol{M}_2\boldsymbol{\Xi}^{n-1} - \frac{dt}{2}\boldsymbol{I}\nabla\boldsymbol{\Xi}^{n-1} + \frac{dt}{2}\boldsymbol{I}\nabla\cdot\zeta(\boldsymbol{x})\nabla\boldsymbol{\Xi}^{n-1} + dt\boldsymbol{R} - dt\boldsymbol{N}\left(\boldsymbol{F}^{n-1} - \widetilde{\boldsymbol{F}}^{n-1}\right).\end{aligned} \tag{2.17}$$

Analogous to Theorem 2.1, we can achieve

$$\left\|\boldsymbol{\Xi}^n\right\|^2_{\boldsymbol{H}_w(\Omega)} \leq \left\{\max_{1\leq m\leq n}\|\boldsymbol{R}\|^2_{\boldsymbol{L}^2(\Omega)}\right\}\exp\left(\frac{2\boldsymbol{L}ndt}{\|D\|}\right) \leq \mathbf{C}dt^2,$$

which completes the proof. ■

3. Interpolating MLS approximation

Let $u^h(x)$ be approximate value of $u(x)$ on Ω. Lancaster and Salkauskas [4] introduced the singular weight function

$$w(x-x_I) = \begin{cases}\|x-x_I\|^{-\alpha}, & \|x-x_I\| \leq \delta,\\ 0, & o.w,\end{cases} \tag{3.1}$$

in which α is an even positive integer. The inner product

$$(f,g)_x = \sum_{I=1}^{n} w(x,x_I)f(x_I)g(x_I), \tag{3.2}$$

is defined for arbitrary functions f and g, and the associated norm is

$$\|f\|_x = \sqrt{(f,f)_x}. \tag{3.3}$$

We use the basis polynomials introduced in [32]. Now, we put

$$q_1(x) = \frac{p_1(x)}{\|p_1(x)\|_x} = \left[\sum_{I=1}^{n} w(x-x_I)\right]^{-\frac{1}{2}}, \tag{3.4}$$

thus the orthogonal basis functions can be defined by

$$q_i(x) = p_i(x) - (p_i,q_1)_x q_1(x) = p_i(x) - \frac{\sum_{I=1}^{n} p_i(x_I)w(x-x_I)}{\sum_{I=1}^{n} w(x-x_I)}, \qquad i = 2,3,\ldots,m, \tag{3.5}$$

in which $q_1(x)$ is orthogonal to $q_i(x)$. Using the orthogonal basis $(q_1,q_2,\ldots,q_m)$ in the IMLS approximation, yields

$$u^h(x) = \mathbf{v}^T(x)\mathbf{u} + \mathbf{b}^T(x)\mathbf{s}(x), \tag{3.6}$$

such that

$$\begin{aligned}
\mathbf{u} &= \begin{bmatrix} u_1 & u_2 & \dots & u_n \end{bmatrix}^{\mathrm{T}},\\
\mathbf{v} &= \begin{bmatrix} v_1(x) & v_2(x) & \dots & v_n(x) \end{bmatrix}^{\mathrm{T}},\\
\mathbf{b}(x) &= \begin{bmatrix} q_2(x) & q_3(x) & \dots & q_m(x) \end{bmatrix}^{\mathrm{T}},\\
\mathbf{s}(x) &= \begin{bmatrix} s_1(x) & s_2(x) & \dots & s_{m-1}(x) \end{bmatrix}^{\mathrm{T}} = \mathbf{A}_x^{-1}\mathbf{B}_x\mathbf{u},
\end{aligned}$$

and

$$v_I(x) = \frac{w(x-x_I)}{\sum_{J=1}^{n} w(x-x_J)}, \qquad \mathbf{A}_x = \mathbf{Q}^T(x)\mathbf{W}(x)\mathbf{Q}(x), \qquad \mathbf{B}_x = \mathbf{Q}^T(x)\mathbf{W}(x), \tag{3.7}$$

$$\mathbf{Q}(x) = \begin{bmatrix} q_2(x_1) & q_3(x_1) & \dots & q_m(x_1)\\ q_2(x_2) & q_3(x_2) & \dots & q_m(x_2)\\ \vdots & \vdots & \ddots & \vdots\\ q_2(x_n) & q_3(x_n) & \dots & q_m(x_n) \end{bmatrix}, \qquad \mathbf{W}(x) = \begin{bmatrix} w(x-x_1) & 0 & \dots & 0\\ 0 & w(x-x_2) & \dots & 0\\ \vdots & \vdots & \ddots & \vdots\\ 0 & 0 & \dots & w(x-x_n) \end{bmatrix}. \tag{3.8}$$

Finally, we can extract these basis functions

$$\Phi^*(x) = \left[\phi_1^*, \phi_2^*, \dots, \phi_n^*\right] = \mathbf{v}^T(x) + \mathbf{b}^T(x)\mathbf{A}_x^{-1}(x)\mathbf{B}_x(x). \tag{3.9}$$

4. Analytical investigation of full-discrete scheme

Before checking the convergence of the IEFG method, we review some preliminaries. We set

$$\omega_r^d = span\left\{\varphi_1, \varphi_2, \dots, \varphi_d\right\}, \tag{4.1}$$

and also we consider the following Ritz-projection

$$\boldsymbol{Q}_h^1 : \omega \to \omega_r, \tag{4.2}$$

such that for $v \in \omega$

$$\left(\nabla \boldsymbol{Q}_h^1 v, \nabla u_r\right) = \left(\nabla v, \nabla u_r\right), \qquad \forall\ u_r \in \omega_r. \tag{4.3}$$

Lemma 1 ([9]). *If $\psi(\boldsymbol{x}) \in C^{m,1}(\Omega)$, then*

$$\exists\ \boldsymbol{C}_\eta > 0, \qquad s.t. \qquad \left\| D^\eta \psi - D^\eta \boldsymbol{Q}_h^1 \psi \right\|_{L^2(\Omega)} \le \boldsymbol{C}_\eta \delta^{m+1-|\eta|} |\psi|_{m,1}.$$

Also, from Eq. (2.3) we have: Find a $\boldsymbol{u}_h^n \in \omega_r^d$ such that

$$\begin{aligned}
\boldsymbol{M}_1 \left\langle \boldsymbol{u}^n, \boldsymbol{v}\right\rangle &+ \frac{dt}{2}\boldsymbol{I}\left\langle D\nabla \boldsymbol{u}^n, \nabla \boldsymbol{v}\right\rangle - \frac{dt}{2}\boldsymbol{I}\left\langle \boldsymbol{u}^n, \frac{\partial}{\partial x}\boldsymbol{v}\right\rangle - \frac{dt}{2}\boldsymbol{I}\left\langle \boldsymbol{u}^n, \frac{\partial}{\partial y}\boldsymbol{v}\right\rangle\\
&= \boldsymbol{M}_2 \left\langle \boldsymbol{u}^{n-1}, \boldsymbol{v}\right\rangle - \frac{dt}{2}\boldsymbol{I}\left\langle D\nabla \boldsymbol{u}^{n-1}, \nabla \boldsymbol{v}\right\rangle + \frac{dt}{2}\boldsymbol{I}\left\langle \boldsymbol{u}^{n-1}, \frac{\partial}{\partial x}\boldsymbol{v}\right\rangle\\
&+ \frac{dt}{2}\boldsymbol{I}\left\langle \boldsymbol{u}^{n-1}, \frac{\partial}{\partial y}\boldsymbol{v}\right\rangle - dt\boldsymbol{N}\left\langle \boldsymbol{F}^{n-1}, \boldsymbol{v}\right\rangle + dt\left\langle \boldsymbol{R}_t^n, \boldsymbol{v}\right\rangle, \qquad \forall\ \ \boldsymbol{v} \in \boldsymbol{H}_0^1(\Omega).
\end{aligned} \tag{4.4}$$

Also, the IEFG formulation is:
Find a $\boldsymbol{U}_h^n \in \omega_r^d$ such that

$$\begin{aligned}
\boldsymbol{M}_1 \left\langle \boldsymbol{U}_h^n, \boldsymbol{v}_h\right\rangle &+ \frac{dt}{2}\boldsymbol{I}\left\langle D\nabla \boldsymbol{U}_h^n, \nabla \boldsymbol{v}_h\right\rangle - \frac{dt}{2}\boldsymbol{I}\left\langle \boldsymbol{U}_h^n, \frac{\partial}{\partial x}\boldsymbol{v}_h\right\rangle - \frac{dt}{2}\boldsymbol{I}\left\langle \boldsymbol{U}_h^n, \frac{\partial}{\partial y}\boldsymbol{v}_h\right\rangle\\
&= \boldsymbol{M}_2 \left\langle \boldsymbol{U}_h^{n-1}, \boldsymbol{v}_h\right\rangle - \frac{dt}{2}\boldsymbol{I}\left\langle D\nabla \boldsymbol{U}_h^{n-1}, \nabla \boldsymbol{v}_h\right\rangle + \frac{dt}{2}\boldsymbol{I}\left\langle \boldsymbol{U}_h^{n-1}, \frac{\partial}{\partial x}\boldsymbol{v}_h\right\rangle\\
&+ \frac{dt}{2}\boldsymbol{I}\left\langle \boldsymbol{U}_h^{n-1}, \frac{\partial}{\partial y}\boldsymbol{v}\right\rangle - dt\boldsymbol{N}\left\langle \boldsymbol{F}^{n-1}, \boldsymbol{v}_h\right\rangle, \qquad \forall\ \ \boldsymbol{v}_h \in \boldsymbol{H}_0^1(\Omega).
\end{aligned} \tag{4.5}$$

Lemma 2. *Let*

$$\left\langle \boldsymbol{\Phi}_h^{1,n}, \boldsymbol{v}\right\rangle = -\boldsymbol{M}_1\left\langle \boldsymbol{Q}_h^1\boldsymbol{u}^n - \boldsymbol{u}^n, \boldsymbol{v}\right\rangle + \frac{dt}{2}\boldsymbol{I}\left\langle \boldsymbol{Q}_h^1\boldsymbol{u}^n - \boldsymbol{u}^n, \frac{\partial}{\partial x}\boldsymbol{v}\right\rangle + \frac{dt}{2}\boldsymbol{I}\left\langle \boldsymbol{Q}_h^1\boldsymbol{u}^n - \boldsymbol{u}^n, \frac{\partial}{\partial y}\boldsymbol{v}\right\rangle$$

$$+ \boldsymbol{M}_2 \left\langle \boldsymbol{Q}_h^1 \boldsymbol{u}^{n-1} - \boldsymbol{u}^{n-1}, \boldsymbol{v} \right\rangle + \frac{dt}{2} \boldsymbol{I} \left\langle \boldsymbol{Q}_h^1 \boldsymbol{u}^{n-1} - \boldsymbol{u}^{n-1}, \frac{\partial}{\partial x} \boldsymbol{v} \right\rangle + \frac{dt}{2} \boldsymbol{I} \left\langle \boldsymbol{Q}_h^1 \boldsymbol{u}^{n-1} - \boldsymbol{u}^{n-1}, \frac{\partial}{\partial y} \boldsymbol{v} \right\rangle,$$

Then, we have

$$\left\| \boldsymbol{\Phi}_h^{1,n} \right\|_{L^2(\Omega)} \leq \boldsymbol{C}(dt + \delta^m).$$

Proof. From Lemma 1, the proof is clear. ■

Theorem 4.1. *Let $\boldsymbol{u}^n$ and $\boldsymbol{U}_h^n$ be solutions of (4.4) and (4.5), respectively. Then*

$$\left\| \boldsymbol{u}^n - \boldsymbol{U}_h^n \right\|_{\boldsymbol{L}^2(\Omega)} \leq \boldsymbol{C}(dt + \delta^m). \tag{4.6}$$

Proof. Subtracting Eq. (4.5) from (4.4), results

$$\begin{aligned}
\boldsymbol{M}_1 \left\langle \boldsymbol{u}^n - \boldsymbol{U}_h^n, \boldsymbol{v} \right\rangle &+ \frac{dt}{2} \boldsymbol{I} \left\langle D\nabla \boldsymbol{u}^n - D\nabla \boldsymbol{U}_h^n, \nabla \boldsymbol{v} \right\rangle \\
&- \frac{dt}{2} \boldsymbol{I} \left\langle \boldsymbol{u}^n - \boldsymbol{U}_h^n, \frac{\partial}{\partial x} \boldsymbol{v} \right\rangle - \frac{dt}{2} \boldsymbol{I} \left\langle \boldsymbol{u}^n - \boldsymbol{U}_h^n, \frac{\partial}{\partial y} \boldsymbol{v} \right\rangle \\
&= \boldsymbol{M}_2 \left\langle \boldsymbol{u}^{n-1} - \boldsymbol{U}_h^{n-1}, \boldsymbol{v} \right\rangle - \frac{dt}{2} \boldsymbol{I} \left\langle D\nabla \boldsymbol{u}^{n-1} - D\nabla \boldsymbol{U}_h^{n-1}, \nabla \boldsymbol{v} \right\rangle \\
&+ \frac{dt}{2} \boldsymbol{I} \left\langle \boldsymbol{u}^{n-1} - \boldsymbol{U}_h^{n-1}, \frac{\partial}{\partial x} \boldsymbol{v} \right\rangle + \frac{dt}{2} \boldsymbol{I} \left\langle \boldsymbol{u}^{n-1} - \boldsymbol{U}_h^{n-1}, \frac{\partial}{\partial y} \boldsymbol{v} \right\rangle \\
&- dt \boldsymbol{N} \left\langle \boldsymbol{F}^{n-1} - \bar{\boldsymbol{F}}^{n-1}, \boldsymbol{v} \right\rangle + dt \left\langle \boldsymbol{R}_t^n, \boldsymbol{v} \right\rangle, \qquad \forall \quad \boldsymbol{v} \in \boldsymbol{H}_0^1(\Omega).
\end{aligned} \tag{4.7}$$

From (4.3), we have

$$\begin{aligned}
\boldsymbol{M}_1 \left\langle \boldsymbol{Q}_h^1 \boldsymbol{u}^n - \boldsymbol{U}_h^n, \boldsymbol{v} \right\rangle &+ \frac{dt}{2} \boldsymbol{I} \left\langle D\nabla \boldsymbol{Q}_h^1 \boldsymbol{u}^n - D\nabla \boldsymbol{U}_h^n, \nabla \boldsymbol{v} \right\rangle \\
&- \frac{dt}{2} \boldsymbol{I} \left\langle \boldsymbol{Q}_h^1 \boldsymbol{u}^n - \boldsymbol{U}_h^n, \frac{\partial}{\partial x} \boldsymbol{v} \right\rangle - \frac{dt}{2} \boldsymbol{I} \left\langle \boldsymbol{Q}_h^1 \boldsymbol{u}^n - \boldsymbol{U}_h^n, \frac{\partial}{\partial y} \boldsymbol{v} \right\rangle \\
&= \boldsymbol{M}_2 \left\langle \boldsymbol{Q}_h^1 \boldsymbol{u}^{n-1} - \boldsymbol{U}_h^{n-1}, \boldsymbol{v} \right\rangle - \frac{dt}{2} \boldsymbol{I} \left\langle D\nabla \boldsymbol{Q}_h^1 \boldsymbol{u}^{n-1} - D\nabla \boldsymbol{U}_h^{n-1}, \nabla \boldsymbol{v} \right\rangle \\
&+ \frac{dt}{2} \boldsymbol{I} \left\langle \boldsymbol{Q}_h^1 \boldsymbol{u}^{n-1} - \boldsymbol{U}_h^{n-1}, \frac{\partial}{\partial x} \boldsymbol{v} \right\rangle + \frac{dt}{2} \boldsymbol{I} \left\langle \boldsymbol{Q}_h^1 \boldsymbol{u}^{n-1} - \boldsymbol{U}_h^{n-1}, \frac{\partial}{\partial y} \boldsymbol{v} \right\rangle \\
&- dt \boldsymbol{N} \left\langle \boldsymbol{F}^{n-1} - \bar{\boldsymbol{F}}^{n-1}, \boldsymbol{v} \right\rangle + dt \left\langle \boldsymbol{R}_t^n, \boldsymbol{v} \right\rangle - \boldsymbol{M}_1 \left\langle \boldsymbol{u}^n - Q_h^1 \boldsymbol{u}^n, \boldsymbol{v} \right\rangle \\
&+ \frac{dt}{2} \boldsymbol{I} \left\langle \boldsymbol{u}^n - \boldsymbol{Q}_h^1 \boldsymbol{u}^n, \frac{\partial}{\partial x} \boldsymbol{v} \right\rangle + \frac{dt}{2} \boldsymbol{I} \left\langle \boldsymbol{u}^n - \boldsymbol{Q}_h^1 \boldsymbol{u}^n, \frac{\partial}{\partial y} \boldsymbol{v} \right\rangle + \boldsymbol{M}_2 \left\langle \boldsymbol{u}^{n-1} - \boldsymbol{Q}_h^1 \boldsymbol{u}^{n-1}, \boldsymbol{v} \right\rangle \\
&+ \frac{dt}{2} \boldsymbol{I} \left\langle \boldsymbol{u}^{n-1} - \boldsymbol{Q}_h^1 \boldsymbol{u}^{n-1}, \frac{\partial}{\partial x} \boldsymbol{v} \right\rangle + \frac{dt}{2} \boldsymbol{I} \left\langle \boldsymbol{u}^{n-1} - \boldsymbol{Q}_h^1 \boldsymbol{u}^{n-1}, \frac{\partial}{\partial y} \boldsymbol{v} \right\rangle, \qquad \forall \boldsymbol{v} \in \boldsymbol{H}_0^1(\Omega).
\end{aligned}$$

By using the definitions

$$\boldsymbol{\Pi}_h^{1,n} = \boldsymbol{Q}_h^1 \boldsymbol{u}^n - \boldsymbol{U}_h^n, \qquad \boldsymbol{\Lambda}_{r,d}^n = \boldsymbol{u}^n - \boldsymbol{Q}_h^1 \boldsymbol{u}^n,$$

the previous relation can be rewritten as

$$\begin{aligned}
\boldsymbol{M}_1 \left\langle \boldsymbol{\Pi}_h^{1,n}, \boldsymbol{v} \right\rangle &+ \frac{dt}{2} \boldsymbol{I} \left\langle D\nabla \boldsymbol{\Pi}_h^{1,n}, \nabla \boldsymbol{v} \right\rangle - \frac{dt}{2} \boldsymbol{I} \left\langle \boldsymbol{\Pi}_h^{1,n}, \frac{\partial}{\partial x} \boldsymbol{v} \right\rangle - \frac{dt}{2} \boldsymbol{I} \left\langle \boldsymbol{\Pi}_h^{1,n}, \frac{\partial}{\partial y} \boldsymbol{v} \right\rangle \\
&= \boldsymbol{M}_2 \left\langle \boldsymbol{\Pi}_h^{1,n-1}, \boldsymbol{v} \right\rangle - \frac{dt}{2} \boldsymbol{I} \left\langle \zeta(\boldsymbol{x}) \nabla \boldsymbol{\Pi}_h^{1,n-1}, \nabla \boldsymbol{v} \right\rangle \\
&+ \frac{dt}{2} \boldsymbol{I} \left\langle \boldsymbol{\Pi}_h^{1,n-1}, \frac{\partial}{\partial x} \boldsymbol{v} \right\rangle + \frac{dt}{2} \boldsymbol{I} \left\langle \boldsymbol{\Pi}_h^{1,n-1}, \frac{\partial}{\partial y} \boldsymbol{v} \right\rangle \\
&- dt \boldsymbol{N} \left\langle \boldsymbol{F}^{n-1} - \bar{\boldsymbol{F}}^{n-1}, \boldsymbol{v} \right\rangle + dt \left\langle \boldsymbol{R}_t^n, \boldsymbol{v} \right\rangle - \boldsymbol{M}_1 \left\langle \boldsymbol{\Lambda}_h^{1,n}, \boldsymbol{v} \right\rangle \\
&+ \frac{dt}{2} \boldsymbol{I} \left\langle \boldsymbol{\Lambda}_h^{1,n}, \frac{\partial}{\partial x} \boldsymbol{v} \right\rangle + \frac{dt}{2} \boldsymbol{I} \left\langle \boldsymbol{\Lambda}_h^{1,n}, \frac{\partial}{\partial y} \boldsymbol{v} \right\rangle + \boldsymbol{M}_2 \left\langle \boldsymbol{\Lambda}_h^{1,n-1}, \boldsymbol{v} \right\rangle \\
&+ \frac{dt}{2} \boldsymbol{I} \left\langle \boldsymbol{\Lambda}_h^{1,n-1}, \frac{\partial}{\partial x} \boldsymbol{v} \right\rangle + \frac{dt}{2} \boldsymbol{I} \left\langle \boldsymbol{\Lambda}_h^{1,n-1}, \frac{\partial}{\partial y} \boldsymbol{v} \right\rangle, \qquad \forall \boldsymbol{v} \in \boldsymbol{H}_0^1(\Omega).
\end{aligned}$$

Thus, by assuming

$$\left\langle \boldsymbol{\Phi}_h^{1,n}, \boldsymbol{v} \right\rangle = -\boldsymbol{M}_1 \left\langle \boldsymbol{\Lambda}_h^{1,n}, \boldsymbol{v} \right\rangle + \frac{dt}{2}\boldsymbol{I}\left\langle \boldsymbol{\Lambda}_h^{1,n}, \frac{\partial}{\partial x}\boldsymbol{v} \right\rangle + \frac{dt}{2}\boldsymbol{I}\left\langle \boldsymbol{\Lambda}_h^{1,n}, \frac{\partial}{\partial y}\boldsymbol{v} \right\rangle + \boldsymbol{M}_2 \left\langle \boldsymbol{\Lambda}_h^{1,n-1}, \boldsymbol{v} \right\rangle + \frac{dt}{2}\boldsymbol{I}\left\langle \boldsymbol{\Lambda}_h^{1,n-1}, \frac{\partial}{\partial x}\boldsymbol{v} \right\rangle + \frac{dt}{2}\boldsymbol{I}\left\langle \boldsymbol{\Lambda}_h^{1,n-1}, \frac{\partial}{\partial y}\boldsymbol{v} \right\rangle,$$

we have

$$\begin{aligned}\boldsymbol{M}_1 \left\langle \boldsymbol{\Pi}_h^{1,n}, \boldsymbol{v} \right\rangle + \frac{dt}{2}\boldsymbol{I}\left\langle \zeta(\boldsymbol{x})\nabla \boldsymbol{\Pi}_h^{1,n}, \nabla \boldsymbol{v} \right\rangle - \frac{dt}{2}\boldsymbol{I}\left\langle \boldsymbol{\Pi}_h^{1,n}, \frac{\partial}{\partial x}\boldsymbol{v} \right\rangle - \frac{dt}{2}\boldsymbol{I}\left\langle \boldsymbol{\Pi}_h^{1,n}, \frac{\partial}{\partial y}\boldsymbol{v} \right\rangle \\ = \boldsymbol{M}_2 \left\langle \boldsymbol{\Pi}_h^{1,n-1}, \boldsymbol{v} \right\rangle - \frac{dt}{2}\boldsymbol{I}\left\langle D\nabla \boldsymbol{\Pi}_h^{1,n-1}, \nabla \boldsymbol{v} \right\rangle + \frac{dt}{2}\boldsymbol{I}\left\langle \boldsymbol{\Pi}_h^{1,n-1}, \frac{\partial}{\partial x}\boldsymbol{v} \right\rangle \\ + \frac{dt}{2}\boldsymbol{I}\left\langle \boldsymbol{\Pi}_h^{1,n-1}, \frac{\partial}{\partial y}\boldsymbol{v} \right\rangle - dt\boldsymbol{N}\left\langle \boldsymbol{F}^{n-1} - \bar{\boldsymbol{F}}^{n-1}, \boldsymbol{v} \right\rangle + dt\left\langle \boldsymbol{R}_t^n, \boldsymbol{v} \right\rangle \\ + \left\langle \boldsymbol{\Phi}_h^{1,n}, \boldsymbol{v} \right\rangle, \quad \forall \boldsymbol{v} \in \boldsymbol{H}_0^1(\Omega).\end{aligned}$$

By setting $\boldsymbol{v}_h = \Xi_{r,d}^n$, we obtain

$$\begin{aligned}\boldsymbol{M}_1 \left\langle \boldsymbol{\Pi}_h^{1,n}, \boldsymbol{\Pi}_h^{1,n} \right\rangle + \frac{dt}{2}\boldsymbol{I}\left\langle D\nabla \boldsymbol{\Pi}_h^{1,n}, \nabla \boldsymbol{\Pi}_h^{1,n} \right\rangle - \frac{dt}{2}\boldsymbol{I}\left\langle \boldsymbol{\Pi}_h^{1,n}, \frac{\partial}{\partial x}\boldsymbol{\Pi}_h^{1,n} \right\rangle - \frac{dt}{2}\boldsymbol{I}\left\langle \boldsymbol{\Pi}_h^{1,n}, \frac{\partial}{\partial y}\boldsymbol{\Pi}_h^{1,n} \right\rangle \\ = \boldsymbol{M}_2 \left\langle \boldsymbol{\Pi}_h^{1,n-1}, \boldsymbol{\Pi}_h^{1,n} \right\rangle - \frac{dt}{2}\boldsymbol{I}\left\langle D\nabla \boldsymbol{\Pi}_h^{1,n-1}, \nabla \boldsymbol{\Pi}_h^{1,n} \right\rangle + \frac{dt}{2}\boldsymbol{I}\left\langle \boldsymbol{\Pi}_h^{1,n-1}, \frac{\partial}{\partial x}\boldsymbol{\Pi}_h^{1,n} \right\rangle \\ + \frac{dt}{2}\boldsymbol{I}\left\langle \boldsymbol{\Pi}_h^{1,n-1}, \frac{\partial}{\partial y}\boldsymbol{\Pi}_h^{1,n} \right\rangle - dt\boldsymbol{N}\left\langle \boldsymbol{F}^{n-1} - \bar{\boldsymbol{F}}^{n-1}, \boldsymbol{\Pi}_h^{1,n} \right\rangle + dt\left\langle \boldsymbol{R}_t^n, \boldsymbol{\Pi}_h^{1,n} \right\rangle + \left\langle \boldsymbol{\Phi}_h^{1,n}, \boldsymbol{\Pi}_h^{1,n} \right\rangle.\end{aligned}$$

Thus, we can write

$$\begin{aligned}\boldsymbol{M}_1 \left\| \boldsymbol{\Pi}_h^{1,n} \right\|_{L^2(\Omega)}^2 + \frac{dt}{2}\boldsymbol{I}\,\|D\| \left\| \nabla \boldsymbol{\Pi}_h^{1,n} \right\|_{L^2(\Omega)}^2 \\ \leq \frac{dt}{2}\boldsymbol{I}\left\langle \boldsymbol{\Pi}_h^{1,n}, \frac{\partial}{\partial x}\boldsymbol{\Pi}_h^{1,n} \right\rangle + \frac{dt}{2}\boldsymbol{I}\left\langle \boldsymbol{\Pi}_h^{1,n}, \frac{\partial}{\partial y}\boldsymbol{\Pi}_h^{1,n} \right\rangle \\ + \boldsymbol{M}_2 \left\| \boldsymbol{\Pi}_h^{1,n-1} \right\| \left\| \boldsymbol{\Pi}_h^{1,n} \right\| + \frac{dt}{2}\boldsymbol{I}\,\|D\| \left\| \nabla \boldsymbol{\Pi}_h^{1,n-1} \right\| \left\| \nabla \boldsymbol{\Pi}_h^{1,n} \right\| \\ + \frac{dt}{2}\boldsymbol{I}\left\langle \boldsymbol{\Pi}_h^{1,n-1}, \frac{\partial}{\partial x}\boldsymbol{\Pi}_h^{1,n} \right\rangle + \frac{dt}{2}\boldsymbol{I}\left\langle \boldsymbol{\Pi}_h^{1,n-1}, \frac{\partial}{\partial y}\boldsymbol{\Pi}_h^{1,n} \right\rangle \\ - dt\boldsymbol{L}\boldsymbol{N} \left\| \boldsymbol{\Pi}_h^{1,n-1} \right\| \left\| \boldsymbol{\Pi}_h^{1,n} \right\| + dt \left\| \boldsymbol{R}_t^n \right\| \left\| \boldsymbol{\Pi}_h^{1,n} \right\| + dt \left\| \boldsymbol{\Phi}_h^{1,n} \right\| \left\| \boldsymbol{\Pi}_h^{1,n} \right\|.\end{aligned}$$

So

$$\begin{aligned}&\frac{1}{2}\boldsymbol{M}_1 \left\| \boldsymbol{\Pi}_h^{1,n} \right\|_{\boldsymbol{L}^2(\Omega)}^2 + \frac{dt}{4}\|D\| \left\| \nabla \boldsymbol{\Pi}_h^{1,n} \right\|_{\boldsymbol{L}^2(\Omega)}^2 \\ &\leq \frac{1}{2}\boldsymbol{M}_1 \left\| \boldsymbol{\Pi}_h^{1,n-1} \right\|_{\boldsymbol{L}^2(\Omega)}^2 + \frac{dt}{4}\|D\| \left\| \nabla \boldsymbol{\Pi}_h^{1,n-1} \right\|_{\boldsymbol{L}^2(\Omega)}^2 + \frac{dt}{2}\left\| \boldsymbol{\Pi}^n \right\|_{\boldsymbol{L}^2(\Omega)} \left\| \nabla \boldsymbol{\Pi}^n \right\|_{\boldsymbol{L}^2(\Omega)} + \frac{dt}{2}\left\| \boldsymbol{\Pi}^{n-1} \right\|_{\boldsymbol{L}^2(\Omega)} \left\| \nabla \boldsymbol{\Pi}^n \right\|_{\boldsymbol{L}^2(\Omega)} \\ &+ \frac{\boldsymbol{C_1}\boldsymbol{L}dt}{2\|D\|} \left\| \boldsymbol{\Pi}_h^{1,n} \right\|_{\boldsymbol{L}^2(\Omega)}^2 + \frac{\boldsymbol{C_2}\boldsymbol{L}dt}{2\|D\|} \left\| \boldsymbol{\Pi}_h^{1,n-1} \right\|_{\boldsymbol{L}^2(\Omega)}^2 \\ &+ \frac{\boldsymbol{C}_3\|D\|}{\boldsymbol{L}}dt \left\| \boldsymbol{R}_t^n \right\|_{L^2(\Omega)}^2 + \frac{\boldsymbol{C_1}\boldsymbol{L}dt}{4\|D\|} \left\| \boldsymbol{\Pi}_h^{1,n} \right\|_{L^2(\Omega)}^2 + \frac{\boldsymbol{C}_3\|D\|}{\boldsymbol{L}}dt \left\| \boldsymbol{\Phi}_h^{1,n} \right\|_{L^2(\Omega)}^2 + \frac{\boldsymbol{C_1}\boldsymbol{L}dt}{4\|D\|} \left\| \boldsymbol{\Pi}_h^{1,n} \right\|_{L^2(\Omega)}^2.\end{aligned} \tag{4.8}$$

Now, Eq. (4.8) can be written as

$$\begin{aligned}\boldsymbol{M}_1 \left\| \boldsymbol{\Pi}_h^{1,n} \right\|_{\boldsymbol{L}^2(\Omega)}^2 + \frac{dt}{2}\|D\| \left\| \nabla \boldsymbol{\Pi}_h^{1,n} \right\|_{\boldsymbol{L}^2(\Omega)}^2 \\ \leq \boldsymbol{M}_1 \left\| \boldsymbol{\Pi}_h^{1,n-1} \right\|_{\boldsymbol{L}^2(\Omega)}^2 + \frac{dt}{2}\|D\| \left\| \nabla \boldsymbol{\Pi}_h^{1,n-1} \right\|_{\boldsymbol{L}^2(\Omega)}^2 \\ + \frac{\boldsymbol{C}_1^*\boldsymbol{L}dt}{\|D\|} \left\| \boldsymbol{\Pi}_h^{1,n} \right\|_{\boldsymbol{L}^2(\Omega)}^2 + \frac{\boldsymbol{C}_2^*\boldsymbol{L}dt}{2\|D\|} \left\| \boldsymbol{\Pi}_h^{1,n-1} \right\|_{\boldsymbol{L}^2(\Omega)}^2 \\ + \frac{\boldsymbol{C}_3\|D\|}{\boldsymbol{L}}dt \left\| \boldsymbol{R}_t^n \right\|_{L^2(\Omega)}^2 + \frac{\boldsymbol{C}_3\|D\|}{\boldsymbol{L}}dt \left\| \boldsymbol{\Phi}_h^{1,n} \right\|_{L^2(\Omega)}^2\end{aligned} \tag{4.9}$$

$$+\frac{dt}{2}C_{\Omega}\left\|\nabla \boldsymbol{\Pi}^{n}\right\|^{2}_{\boldsymbol{L}^{2}(\Omega)}+\frac{dt}{4}C_{\Omega}\left\|\nabla \boldsymbol{\Pi}^{n-1}\right\|^{2}_{\boldsymbol{L}^{2}(\Omega)}+\frac{dt}{4}C_{\Omega}\left\|\nabla \boldsymbol{\Pi}^{n}\right\|^{2}_{\boldsymbol{L}^{2}(\Omega)}.$$

From Eq. (4.9) we arrive at

$$\begin{aligned}
&\sum_{m=1}^{n}\left\|\boldsymbol{\Pi}_{h}^{1,m}\right\|^{2}_{L^{2}(\Omega)}+\frac{dt}{2}\|D\|\sum_{m=1}^{n}\left\|\nabla\boldsymbol{\Pi}_{h}^{1,m}\right\|^{2}_{L^{2}(\Omega)}\\
&\quad\le\sum_{m=1}^{n}\left\|\boldsymbol{\Pi}_{h}^{1,m-1}\right\|^{2}_{L^{2}(\Omega)}+\frac{dt}{2}\|D\|\sum_{m=1}^{n}\left\|\nabla\boldsymbol{\Pi}_{h}^{1,m-1}\right\|^{2}_{L^{2}(\Omega)}\\
&\quad+\frac{\boldsymbol{C}_{\boldsymbol{1}}^{*}\boldsymbol{L}dt}{\|D\|}\sum_{m=1}^{n}\left\|\boldsymbol{\Pi}_{h}^{1,m}\right\|^{2}_{L^{2}(\Omega)}+\frac{\boldsymbol{C}_{\boldsymbol{2}}^{*}\boldsymbol{L}dt}{2\|D\|}\sum_{m=1}^{n}\left\|\boldsymbol{\Pi}_{h}^{1,m-1}\right\|^{2}_{L^{2}(\Omega)}\\
&\quad+\frac{\boldsymbol{C}_{3}\|D\|}{\boldsymbol{L}}dt\sum_{m=1}^{n}\left\|\boldsymbol{R}_{t}^{m}\right\|^{2}_{L^{2}(\Omega)}+\frac{\boldsymbol{C}_{3}\|D\|}{\boldsymbol{L}}dt\sum_{m=1}^{n}\left\|\boldsymbol{\Phi}_{h}^{1,m}\right\|^{2}_{L^{2}(\Omega)}+dtC_{\Omega}\sum_{m=1}^{n}\left\|\nabla\boldsymbol{\Pi}^{m}\right\|^{2}_{\boldsymbol{L}^{2}(\Omega)}.
\end{aligned}$$

Applying the definition

$$\left\|\boldsymbol{\Pi}_{h}^{1,n}\right\|^{2}_{\boldsymbol{H}_{w}(\Omega)}=\boldsymbol{M}_{1}\left\|\boldsymbol{\Pi}_{h}^{1,n}\right\|^{2}_{\boldsymbol{L}^{2}(\Omega)}+\frac{dt}{2}\|D\|\left\|\nabla\boldsymbol{\Pi}_{h}^{1,n}\right\|^{2}_{\boldsymbol{L}^{2}(\Omega)},$$

and applying the Gronwall Lemma to Eq. (4.10) results in

$$\begin{aligned}
\left\|\boldsymbol{\Pi}_{h}^{1,n}\right\|^{2}_{\boldsymbol{H}_{\omega}(\Omega)}&\le\frac{C\boldsymbol{L}dt}{\|D\|}\sum_{m=1}^{n}\left\|\boldsymbol{\Pi}_{h}^{1,m}\right\|^{2}_{\boldsymbol{H}_{\omega}(\Omega)}+Cdt\sum_{m=1}^{n}\left\|\boldsymbol{R}_{t}^{m}\right\|^{2}_{L^{2}(\Omega)}+Cdt\sum_{m=1}^{n}\left\|\boldsymbol{\Phi}_{h}^{1,m}\right\|^{2}_{L^{2}(\Omega)}+dtC_{\Omega}\sum_{m=1}^{n}\left\|\nabla\boldsymbol{\Pi}^{m}\right\|^{2}_{\boldsymbol{L}^{2}(\Omega)}\\
&\le\frac{C\boldsymbol{L}dt}{\|D\|}\sum_{m=1}^{n}\left\|\boldsymbol{\Pi}_{h}^{1,m}\right\|^{2}_{L^{2}(\Omega)}+Cndt\left\|\boldsymbol{R}_{t}^{m}\right\|^{2}_{L^{2}(\Omega)}+Cndt\left\|\boldsymbol{\Phi}_{h}^{1,m}\right\|^{2}_{L^{2}(\Omega)}+dtC_{\Omega}\sum_{m=1}^{n}\left\|\nabla\boldsymbol{\Pi}^{m}\right\|^{2}_{\boldsymbol{L}^{2}(\Omega)}\\
&\le\left[Cndt\left\|\boldsymbol{R}_{t}^{m}\right\|^{2}_{L^{2}(\Omega)}+Cndt\left\|\boldsymbol{\Phi}_{h}^{1,m}\right\|^{2}_{L^{2}(\Omega)}+dtC_{\Omega}\sum_{m=1}^{n}\left\|\nabla\boldsymbol{\Pi}^{m}\right\|^{2}_{\boldsymbol{L}^{2}(\Omega)}\right]\exp\left(\frac{C\boldsymbol{L}ndt}{\|D\|}\right)\\
&\le\left[CTdt^{2}+Cndt\left(dt^{2}+\delta^{-m}\right)+dtC_{\Omega}\sum_{m=1}^{n}\left\|\nabla\boldsymbol{\Pi}^{m}\right\|^{2}_{\boldsymbol{L}^{2}(\Omega)}\right]\exp\left(\frac{C\boldsymbol{L}T}{\|D\|}\right)\\
&\le C\left(dt^{2}+\delta^{-m}\right)^{2}+dtC_{\Omega}\sum_{m=1}^{n}\left\|\nabla\boldsymbol{\Pi}^{m}\right\|^{2}_{\boldsymbol{L}^{2}(\Omega)}.
\end{aligned}$$

Since in $H_{0}^{k}(\Omega)$ the norm $\|\bullet\|_{L^{k}(\Omega)}$ and the seminorm $|\bullet|_{H^{k}(\Omega)}$ are equivalent, by using the Gronwall inequality we have

$$\left\|\boldsymbol{\Pi}_{h}^{1,n}\right\|_{\boldsymbol{L}^{2}(\Omega)}\le\left\|\boldsymbol{\Pi}_{h}^{1,n}\right\|_{\boldsymbol{H}_{w}(\Omega)}\le C(dt+\delta^{m}).\quad\blacksquare \tag{4.10}$$

5. Numerical results

Here, we give three examples to check the accuracy and the efficiency of the proposed numerical procedure. We survey the theoretical results with the numerical values. In this section, we verify that the theoretical orders are close to the computational orders by using the following formula

$$Ratio=\log_{2}\left(\frac{E(h,2dt)}{E(h,dt)}\right),\qquad E(h,dt)=L_{\infty}(\mathbf{U}_{\text{Approximation}}-\mathbf{u}_{\text{Exact}}).$$

In the current paper, let $\mathbf{X}=\{\mathbf{x}_{i}\}_{i=1}^{N}$ be a set of scattered data in $\Omega\subset\mathbb{R}^{n}$ with fill distance

$$h_{X,\Omega}=\sup_{x\in\Omega}\min_{1\le j\le N}\left\|\varsigma-\varsigma_{j}\right\|_{2}. \tag{5.1}$$

The radius of the weight function is $r=2.7h_{X,\Omega}$. We employ the Gauss–Legendre–Lobatto quadrature with 16 integration nodes to compute the appeared integrals in the weak forms.

Table 1
Results obtained based on the IEFG method for Example 1.

dt	$T = 0.1$		$T = 1$		$T = 2$		CPU time
	L_∞	*Ratio*	L_∞	*Ratio*	L_∞	*Ratio*	
0.1	2.4201×10^{-2}	–	1.5714×10^{-3}	–	1.4041×10^{-4}	–	5.31
0.05	1.4321×10^{-2}	0.75	9.2213×10^{-4}	0.76	8.2310×10^{-5}	0.77	15.11
0.01	8.3782×10^{-3}	0.77	5.4139×10^{-4}	0.79	4.8231×10^{-5}	0.77	38.41
0.005	4.8520×10^{-3}	0.78	3.1241×10^{-4}	0.79	2.7140×10^{-5}	0.82	80.01
0.0025	2.5142×10^{-3}	0.94	1.6347×10^{-5}	0.93	1.4350×10^{-5}	0.91	171.43
0.0013	1.2821×10^{-3}	0.97	8.4241×10^{-5}	0.93	7.3234×10^{-6}	0.97	255.63
0.000625	6.4341×10^{-4}	0.99	4.3238×10^{-5}	0.96	3.7164×10^{-6}	0.98	487.46
0.00031250	3.2174×10^{-4}	1.00	2.1275×10^{-5}	1.02	1.8574×10^{-6}	1.00	866.33

5.1. Example 1 (accuracy test)

For the first example, we study [47,50]

$$\begin{cases} \dfrac{\partial u}{\partial t} + \left(\dfrac{\partial u}{\partial x} + \dfrac{\partial u}{\partial y}\right) - D\left(\dfrac{\partial^2 u}{\partial x^2} + \dfrac{\partial^2 u}{\partial y^2}\right) + 0.6\varpi_p \dfrac{uv}{(1+u)(v+2)} = f(x,y,t), \\ \dfrac{\partial v}{\partial t} + \left(\dfrac{\partial v}{\partial x} + \dfrac{\partial v}{\partial y}\right) - D\left(\dfrac{\partial^2 v}{\partial x^2} + \dfrac{\partial^2 v}{\partial y^2}\right) + 0.6\varpi_p \dfrac{uv}{(1+u)(v+2)} = g(x,y,t), \\ \dfrac{\partial w}{\partial t} + \left(\dfrac{\partial w}{\partial x} + \dfrac{\partial w}{\partial y}\right) - D\left(\dfrac{\partial^2 w}{\partial x^2} + \dfrac{\partial^2 w}{\partial y^2}\right) + 0.6\varpi_p \dfrac{uv}{(1+u)(v+2)} + 2w = h(x,y,t), \end{cases} \tag{5.2}$$

in which $D = 10^{-3}$ and initial conditions are

$$u_0 = v_0 = w_0 = \sin(\pi x)\sin(\pi y),$$

and with zero Dirichlet boundary conditions. Let the exact solutions be

$$u(x,y,t) = e^{-5t}\sin(\pi x)\sin(\pi y), \quad v(x,y,t) = e^{-2t}\sin(\pi x)\sin(\pi y), \quad w(x,y,t) = e^{-3t}\sin(\pi x)\sin(\pi y).$$

Furthermore

$$\begin{aligned} f(x,y,t) &= \pi e^{-5t}\cos(\pi x)\sin(\pi y) - 5e^{-5t}\sin(\pi x)\sin(\pi y) \\ &+ \pi e^{-5t}\cos(\pi y)\sin(\pi x) + 2D\pi^2 e^{-5t}\sin(\pi x)\sin(\pi y) + \\ &+ \frac{3e^{-10t}\sin(\pi x)^3\sin(\pi y)^3}{5\left(e^{-2t}\sin(\pi x)\sin(\pi y)+2\right)\left(e^{-5t}\sin(\pi x)\sin(\pi y)+1\right)}, \\ g(x,y,t) &= \pi e^{-2t}\cos(\pi x)\sin(\pi y) - 2e^{-2t}\sin(\pi x)\sin(\pi y) \\ &+ \pi e^{-2t}\cos(\pi y)\sin(\pi x) + 2D\pi^2 e^{-2t}\sin(\pi x)\sin(\pi y) \\ &+ \frac{e^{-10t}\sin(\pi x)^3\sin(\pi y)^3}{10\left(e^{-2t}\sin(\pi x)\sin(\pi y)+2\right)\left(e^{-5t}\sin(\pi x)\sin(\pi y)+1\right)}, \\ h(x,y,t) &= \pi e^{-3t}\cos(\pi x)\sin(\pi y) - e^{-3t}\sin(\pi x)\sin(\pi y) \\ &+ \pi e^{-3t}\cos(\pi y)\sin(\pi x) + 2D\pi^2 e^{-3t}\sin(\pi x)\sin(\pi y) \\ &+ \frac{4e^{-10t}\sin(\pi x)^3\sin(\pi y)^3}{5\left(e^{-2t}\sin(\pi x)\sin(\pi y)+2\right)\left(e^{-5t}\sin(\pi x)\sin(\pi y)+1\right)}. \end{aligned}$$

We consider this example to check out the theoretical results. Table 1 displays the error and convergence rate acquired using the IEFG method for Example 1. In Table 2, we reported numerical results based on the finite volume method [47] compared with the numerical results of the present method. Fig. 1 shows the graphs of error based on the EFG and IEFG techniques for Example 1. From Fig. 1, we can see that the IEFG method is more stable than the EFG method.

5.2. Example 2

We investigate the following model [47]

$$\begin{cases} \dfrac{\partial u}{\partial t} + \mu\dfrac{\partial u}{\partial x} - D\dfrac{\partial^2 u}{\partial x^2} + \mu\dfrac{\partial u}{\partial y} - D\dfrac{\partial^2 u}{\partial y^2} + 0.6\varpi_p \dfrac{uv}{(1+u)(v+2)} = 0, \\ \dfrac{\partial v}{\partial t} + \mu\dfrac{\partial v}{\partial x} - D\dfrac{\partial^2 v}{\partial x^2} + \mu\dfrac{\partial v}{\partial y} - D\dfrac{\partial^2 v}{\partial y^2} + 0.6\varpi_p \dfrac{uv}{(1+u)(v+2)} = 0, \\ \dfrac{\partial w}{\partial t} + \mu\dfrac{\partial w}{\partial x} - D\dfrac{\partial^2 w}{\partial x^2} + \mu\dfrac{\partial w}{\partial y} - D\dfrac{\partial^2 w}{\partial y^2} + 0.6\varpi_p \dfrac{uv}{(1+u)(v+2)} + 2w = 0, \end{cases} \tag{5.3}$$

Table 2
Comparison between the obtained numerical results.

Finite volume method [47]				
H	h	$\|e_u\|$	$\|e_v\|$	$\|e_w\|$
1/2	1/8	1.841×10^{-2}	1.407×10^{-2}	8.433×10^{-3}
1/3	1/27	5.226×10^{-3}	4.146×10^{-3}	2.443×10^{-3}
1/4	1/64	2.057×10^{-3}	1.723×10^{-3}	1.015×10^{-3}
1/5	1/125	1.190×10^{-3}	8.673×10^{-4}	5.141×10^{-4}
Present method				
Number of collocation points		$\|e_u\|$	$\|e_v\|$	$\|e_w\|$
20		1.110×10^{-2}	1.521×10^{-2}	9.131×10^{-3}
40		8.413×10^{-3}	7.791×10^{-3}	3.889×10^{-3}
80		3.521×10^{-3}	2.551×10^{-3}	1.503×10^{-3}
160		1.280×10^{-3}	9.188×10^{-4}	7.010×10^{-4}

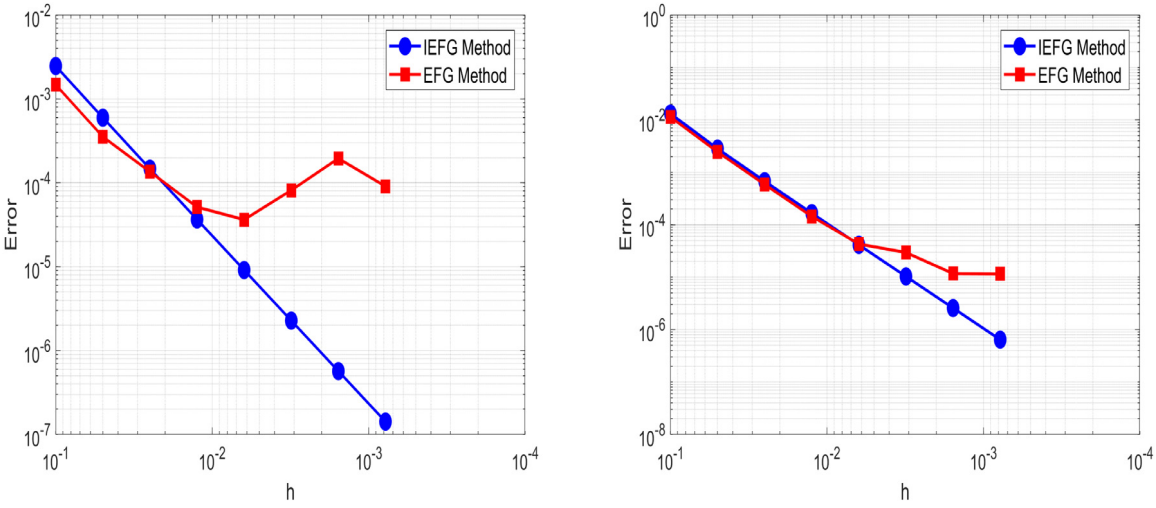

Fig. 1. Diagrams of error for the EFG and IEFG techniques for Example 1.

in which $\mu = [\mu_x, \mu_y] = [1, 1]$ and $D = 10^{-4}$ and zero Dirichlet boundary conditions. The groundwater model is a system of nonlinear equations that it explains how to remove pollutants of groundwater [47]. Eq. (5.3) is an advection–diffusion equation in which the coefficients of advection and diffusion are $\mu = [\mu_x, \mu_y] = [1, 1]$ and $D = 10^{-4}$, respectively. Now, we consider two initial conditions that they are near to the real world problems as

$$u(x, y, 0) = v(x, y, 0) = w(x, y, 0) = x(1 - x)y(1 - y), \tag{5.4}$$

and

$$u(x, y, 0) = v(x, y, 0) = w(x, y, 0) = \delta(0, 0). \tag{5.5}$$

Relations (5.5) and (5.5) are smooth and non-smooth initial data, respectively. Fig. 2 demonstrates the contour of approximation solution based on the component u and initial data (5.4) for Example 2.

Now, we consider initial date (5.4). The current example is very close to the experimentally test problems. The initial conditions for the considered example are based on the delta function. The delta function is a discontinuous function thus the initial condition is not smooth. We solve this case of groundwater model by using the proposed numerical procedure. Figs. 3 and 4 illustrate the contour of approximation solution based on the component u at different values of final time for Example 2. Eq. (1.1) is a system of nonlinear advection–reaction–diffusion equations. The studied model has been proposed to simulate the prevention of groundwater contamination. Figs. 3 and 4 express that the pollution at the initial time has been moved to out of the study region.

6. Conclusion

We proposed a novel meshless numerical procedure to analyze and simulate groundwater equation. The numerical procedure is based on an improvement of the EFG method, e.g. interpolating EFG (IEFG) technique. The IEFG technique is more stable than the classic EFG that this fact has been shown in the numerical results. The stability and convergence of

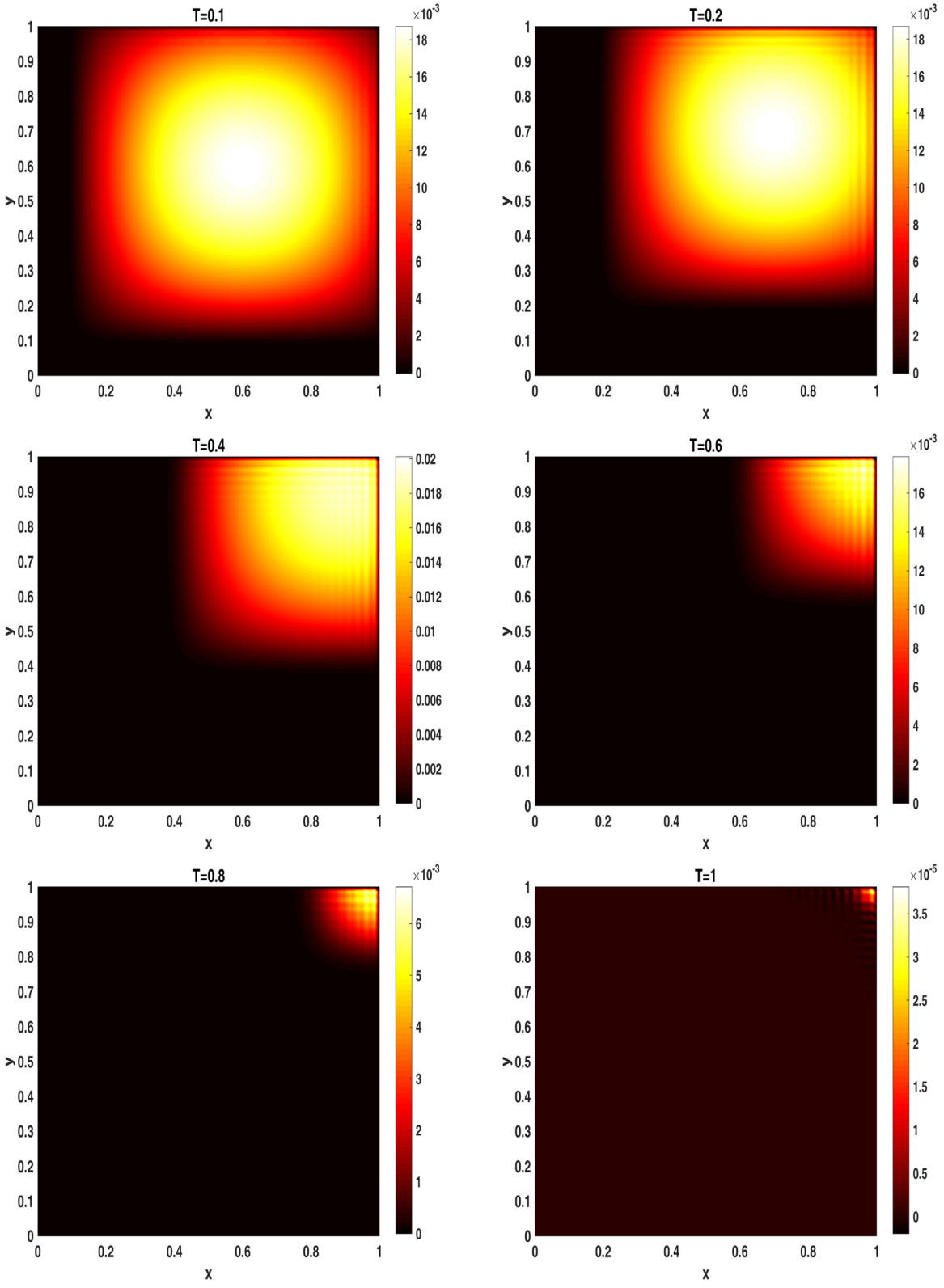

Fig. 2. Contour of approximation solution based on the component u for Example 2.

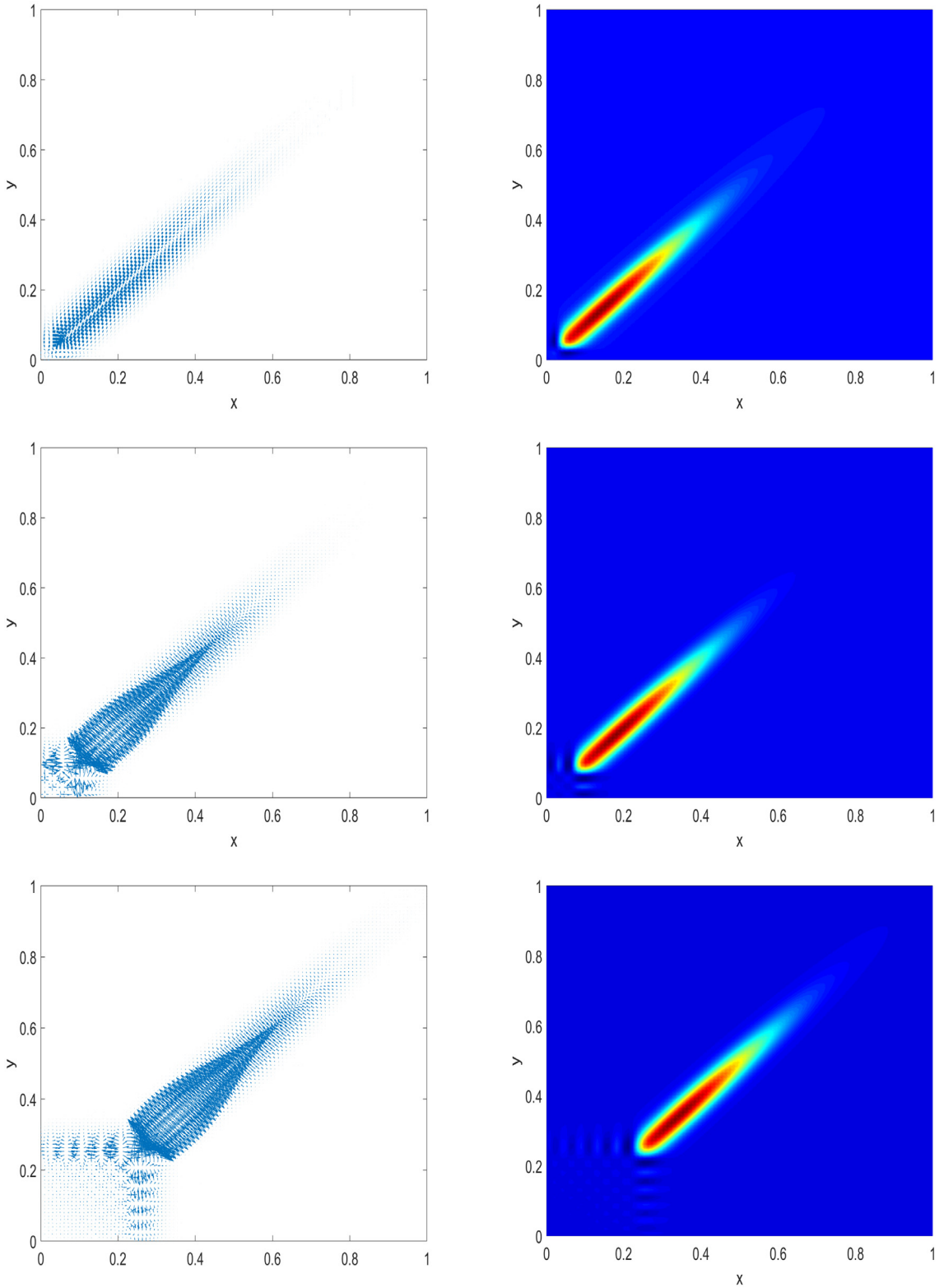

Fig. 3. Contour of approximation solution based on the component u for Example 3.

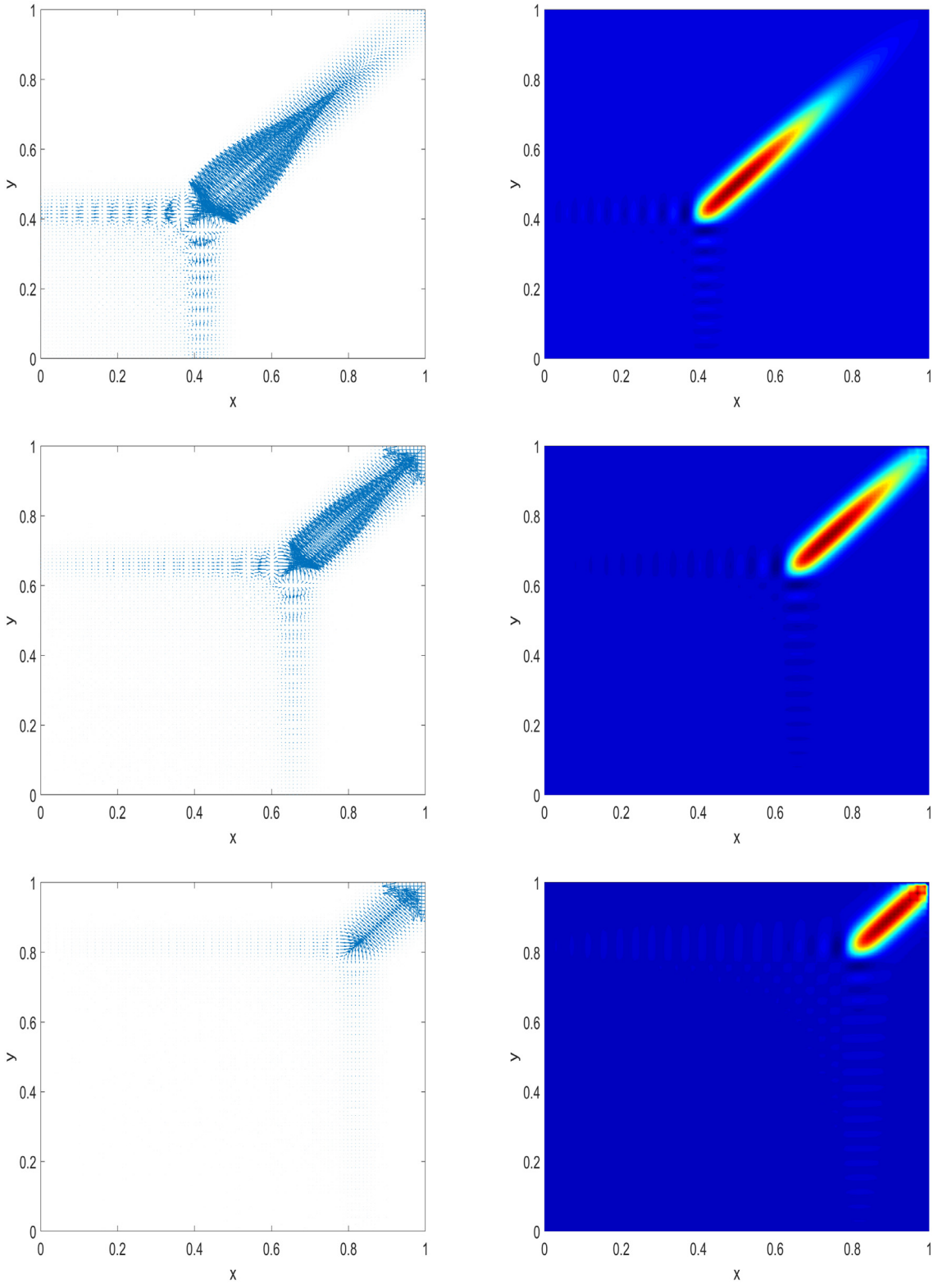

Fig. 4. Contour of approximation solution based on the component u for Example 3.

the new numerical formulation have been investigated. Also, we analyzed the existence and uniqueness of the full-discrete scheme. The computational results confirm the capability of the present scheme in our investigation.

Acknowledgments

The authors are very grateful to the reviewers for carefully reading this paper and for their comments and suggestions which improved the paper. Amirreza Khodadadian and Clemens Heitzinger acknowledge support by FWF (Austrian Science Fund) START Project No. Y660 PDE Models for Nanotechnology.

References

[1] T. Belytschko, Y.Y. Lu, L. Gu, Element free Galerkin methods, Internat. J. Numer. Methods Engrg. 37 (1994) 229–256.
[2] T. Belytschko, Y. Krongauz, D. Organ, M. Fleming, P. Krysl, Meshless methods: An overview and recent developments, Comput. Methods Appl. Mech. Engrg. 139 (1996) 3–47.
[3] H.J. Chung, T. Belytschko, An error estimate in the EFG method, Comput. Mech. 21 (1998) 91–100.
[4] P. Lancaster, K. Salkauskas, Surfaces generated by moving least squares methods, Math. Comp. 37 (155) (1981) 141–158.
[5] H.P. Ren, W. Zhang, An improved boundary element-free method (IBEFM) for two-dimensional potential problems, Chin. Phys. B 18 (10) (2009) 4065–4073.
[6] H.P. Ren, Y.M. Cheng, W. Zhang, An interpolating boundary element-free method (IBEFM) for elasticity problems, Sci. China Phys. Mech. Astron. 53 (4) (2010) 758–766.
[7] F. Sun, J. Wang, Y.M. Cheng, An improved interpolating element-free Galerkin method for elasticity, Chin. Phys. B 22 (12) (2013) 120–203.
[8] J. Wang, J. Wang, F. Sun, Y.M. Cheng, An interpolating boundary element-free method with nonsingular weight function for two–dimensional potential problems, Int. J. Comput. Methods 10 (2013) 1350043.
[9] J. Wang, F. Sun, Y.M. Cheng, A. Huang, Error estimates for the interpolating moving least–squares method, Appl. Math. Comput. 245 (2014) 321–342.
[10] F. Sun, J. Wang, Y.M. Cheng, A. Huang, Error estimates for the interpolating moving least-squares method in n–dimensional space, Appl. Numer. Math. 98 (2015) 79–105.
[11] H.P. Ren, J. Cheng, A. Huang, The complex variable interpolating moving least-squares method, Appl. Math. Comput. 219 (2012) 1724–1736.
[12] Y.M. Cheng, F. Bai, M. Peng, A novel interpolating element-free Galerkin (IEFG) method for two-dimensional elastoplasticity, Appl. Math. Model. 38 (21) (2014) 5187–5197.
[13] Y. Deng, C. Liu, M. Peng, Y.M. Cheng, The interpolating complex variable element-free Galerkin method for temperature field problems, Int. J. Appl. Mech. 7 (2015) 1550017.
[14] Y.M. Cheng, F. Bai, C. Liu, M. Peng, Analyzing nonlinear large deformation with an improved element-free Galerkin method via the interpolating moving least-squares method, Int. J. Comput. Mater. Sci. Eng. 5 (2016) 1650023.
[15] K.M. Liew, Y.M. Cheng, Complex variable boundary element-free method for two-dimensional elastodynamic problems, Comput. Methods Appl. Mech. Eng. 198 (2009) 3925–3933.
[16] L. Chen, Y.M. Cheng, The complex variable reproducing kernel particle method for bending problems of thin plates on elastic foundations, Comput. Mech. 62 (2018) 67–80.
[17] Z.J. Meng, H. Cheng, L.D. Ma, Y.M. Cheng, The dimension split element-free Galerkin method for three-dimensional potential problems, Acta Mech. Sin. 34 (3) (2018) 462–474.
[18] M. Dehghan, M. Abbaszadeh, Variational multiscale element-free Galerkin method combined with the moving kriging interpolation for solving some partial differential equations with discontinuous solutions, Comput. Appl. Math. 37 (3) (2018) 3869–3905.
[19] F.B. Liu, Y.M. Cheng, The improved element-free Galerkin method based on the nonsingular weight functions for elastic large deformation problems, Int. J. Comput. Mater. Sci. Eng. 7 (3) (2018) 1850023.
[20] F.B. Liu, Y.M. Cheng, The improved element-free Galerkin method based on the nonsingular weight functions for inhomogeneous swelling of polymer gels, Int. J. Appl. Mech. 10 (4) (2018) 1850047.
[21] F.B. Liu, Q. Wu, Y.M. Cheng, A meshless method based on the nonsingular weight functions for elastoplastic large deformation problems, Int. J. Appl. Mech. 11 (1) (2019) 1950006.
[22] S. Feng-Xin, W. Ju-Feng, C. Yu-Min, An improved interpolating element-free Galerkin method for elasticity, Chin. Phys. B 22 (12) (2013) 120203.
[23] W. Ju-Feng, S. Feng-Xin, C. Yu-Min, An improved interpolating element-free Galerkin method with a nonsingular weight function for two-dimensional potential problems, Chin. Phys. B 21 (9) (2012) 090204.
[24] H. Ren, Y. Cheng, The interpolating element-free Galerkin (IEFG) method for two-dimensional potential problems, Eng. Anal. Bound. Elem. 36 (5) (2012) 873–880.
[25] D. Li, F. Bai, Y. Cheng, K.M. Liew, A novel complex variable element-free Galerkin method for two-dimensional large deformation problems, Comput. Methods Appl. Mech. Eng. 233 (2012) 1–10.
[26] N. Zhao, H. Ren, The interpolating element-free Galerkin method for 2D transient heat conduction problems, Math. Probl. Eng. 2014 (2014) Article ID 712834, 9 pages.
[27] M. Dehghan, M. Abbaszadeh, Proper orthogonal decomposition variational multiscale element free Galerkin (POD–VMEFG) meshless method for solving incompressible Navier–Stokes equation, Comput. Methods Appl. Mech. Engrg. 311 (2016) 856–888.
[28] X. Li, A meshless interpolating Galerkin boundary node method for Stokes flows, Eng. Anal. Bound. Elem. 51 (2015) 112–122.
[29] L. Zhang, Y. Deng, K.M. Liew, Y. Cheng, The improved complex variable element–free Galerkin method for two-dimensional Schrodinger equation, Comput. Math. Appl. 68 (10) (2014) 1093–1106.
[30] L. Zhang, Y. Deng, K.M. Liew, An improved element–free Galerkin method for numerical modeling of the biological population problems, Eng. Anal. Bound. Elem. 40 (2014) 181–188.
[31] D. Li, Z. Zhang, K.M. Liew, A numerical framework for two-dimensional large deformation of inhomogeneous swelling of gels using the improved complex variable element-free Galerkin method, Comput. Methods Appl. Mech. Eng. 274 (2014) 84–102.
[32] X. Li, Q. Wang, Analysis of the inherent instability of the interpolating moving least squares method when using improper polynomial bases, Eng. Anal. Bound. Elem. 73 (2016) 21–34.
[33] M. Abbaszadeh, M. Dehghan, Numerical and analytical investigations for neutral delay fractional damped diffusion-wave equation based on the stabilized interpolating element free Galerkin (IEFG) method, Appl. Numer. Math. 145 (2019) 488–506.
[34] M. Abbaszadeh, M. Dehghan, The interpolating element-free Galerkin method for solving Korteweg de Vries–Rosenau–regularized long–wave equation with error analysis, Nonlinear Dynam. 96 (2019) 1345–1365.

[35] M. Dehghan, M. Abbaszadeh, Error analysis and numerical simulation of magnetohydrodynamics (MHD) equation based on the interpolating element free Galerkin (IEFG) method, Appl. Numer. Math. 137 (2019) 252–273.
[36] M. Dehghan, M. Abbaszadeh, A. Mohebbi, Analysis of two methods based on Galerkin weak form for fractional diffusion-wave: Meshless interpolating element free Galerkin (IEFG) and finite element methods, Eng. Anal. Bound. Elem. 64 (2016) 205–221.
[37] M. Abbaszadeh, M. Dehghan, The two–grid interpolating element free Galerkin (TG–IEFG) method for solving Rosenau–regularized long wave (RRLW) equation with error analysis, Appl. Anal. 97 (2018) 1129–1153.
[38] M. Dehghan, M. Abbaszadeh, Interpolating stabilized moving least squares (MLS) approximation for 2D elliptic interface problems, Comput. Methods Appl. Mech. Engrg. 328 (2018) 775–803.
[39] M. Dehghan, M. Abbaszadeh, An upwind local radial basis functions-differential quadrature (RBF-DQ) method with proper orthogonal decomposition (POD) approach for solving compressible Euler equation, Eng. Anal. Bound. Elem. 92 (2018) 244–256.
[40] D. Mirzaei, R. Schaback, M. Dehghan, On generalized moving least squares and diffuse derivatives, IMA J. Numer. Anal. 32 (2012) 983–1000.
[41] R. Salehi, M. Dehghan, A generalized moving least square reproducing kernel method, J. Comput. Appl. Math. 249 (2013) 120–132.
[42] R. Salehi, M. Dehghan, A moving least square reproducing polynomial meshless method, Appl. Numer. Math. 69 (2013) 34–58.
[43] Y.-C. Hon, B. Šarler, D.-f. Yun, Local radial basis function collocation method for solving thermo-driven fluid-flow problems with free surface, Eng. Anal. Bound. Elem. 57 (2015) 2–8.
[44] Q. Li, S. Chen, X. Luo, Steady heat conduction analyses using an interpolating element-free Galerkin scaled boundary method, Appl. Math. Comput. 300 (2017) 103–115.
[45] K. Mramor, R. Vertnik, B. Šarler, Simulation of laminar backward facing step flow under magnetic field with explicit local radial basis function collocation method, Eng. Anal. Bound. Elem. 49 (2014) 37–47.
[46] H.E. Kobus, W. Kinzelbach, Contaminant Transport in Groundwater: Proceedings of an international symposium, Stuttgart, 4–6 1989, vol. 3, CRC Press, 1989.
[47] W. Liu, J. Huang, X. Long, Coupled nonlinear advection–diffusion–reaction system for prevention of groundwater contamination by modified upwind finite volume element method, Comput. Math. Appl. 69 (6) (2015) 477–493.
[48] A. Tambue, An exponential integrator for finite volume discretization of a reaction–advection–diffusion equation, Comput. Math. Appl. 71 (9) (2016) 1875–1897.
[49] A.-M. Wazwaz, Partial Differential Equations and Solitary Waves Theory, Springer Science & Business Media, 2010.
[50] M. Ilati, M. Dehghan, Remediation of contaminated groundwater by meshless local weak forms, Comput. Math. Appl. 72 (9) (2016) 2408–2416.
[51] S.A. Sarra, A local radial basis function method for advection–diffusion–reaction equations on complexly shaped domains, Appl. Math. Comput. 218 (19) (2012) 9853–9865.
[52] L. Budinski, J. Fabian, M. Stipić, Lattice Boltzmann method for groundwater flow in non-orthogonal structured lattices, Comput. Math. Appl. 70 (10) (2015) 2601–2615.
[53] B. D'Acunto, F. Parente, G. Urciuoli, Numerical models for 2d free boundary analysis of groundwater in slopes stabilized by drain trenches, Comput. Math. Appl. 53 (10) (2007) 1615–1626.
[54] T. Jiang, Y.-T. Zhang, Krylov implicit integration factor weno methods for semilinear and fully nonlinear advection–diffusion–reaction equations, J. Comput. Phys. 253 (2013) 368–388.
[55] B. Liu, An error analysis of a finite element method for a system of nonlinear advection–diffusion–reaction equations, Appl. Numer. Math. 59 (8) (2009) 1947–1959.
[56] X. Wang, Z. Huo, S. Feng, P. Guo, H. Guan, Estimating groundwater evapotranspiration from irrigated cropland incorporating root zone soil texture and moisture dynamics, J. Hydrol. 543 (2016) 501–509.
[57] W. Zhang, H. Yang, L. Fang, P. Cui, Z. Fang, Study on heat transfer of pile foundation ground heat exchanger with three–dimensional groundwater seepage, Int. J. Heat Mass Transfer 105 (2017) 58–66.
[58] S.M.H.J. Shoushtari, N. Cartwright, P. Perrochet, P. Nielsen, Two–dimensional vertical moisture–pressure dynamics above groundwater waves: Sand flume experiments and modelling, J. Hydrol. 544 (2017) 467–478.